UNIVERSITY OF OKLAHOMA

GRADUATE COLLEGE

THE BEHAVIOR OF EMULSION IN ARTIFICIAL LIFT SYSTEMS

A THESIS

SUBMITTED TO THE GRADUATE FACULTY

in partial fulfillment of the requirements for the

Degree of

MASTER OF SCIENCE

By

EIMAN AL MUNIF
Norman, Oklahoma
2016

THE BEHAVIOR OF EMULSION IN ARTIFICIAL LIFT SYSTEMS

A THESIS APPROVED FOR THE
MEWBOURNE SCHOOL OF PETROLEUM AND GEOLOGICAL ENGINEERING

BY

_____
Dr. Mashhad Fahes, Chair

_____
Dr. Catalin Teodoriu

_____
Dr. Maysam Pournik

I dedicate this thesis to my family and friends for all their support throughout this study. To my father and mother for being the greatest and most inspiring and loving parents. To each special person in my life for always having faith in me and pushing me to be successful as a person and professional.

To God for allowing me to pursue this aspiration, all my accomplishment is because of Him.

Acknowledgements

To begin with, I would like to thank my chair professor Dr. Mashhad Fahes for always being there for me when I had questions regarding my thesis or my work in general, for always giving me answers when I had concerns and for being a kind advisor to me and has always given me good suggestions to attain the best results in. I would also like to thank my committee professor Catailin Teodoriu, who has also been helpful and assist me with my work, and Dr. Maysam Pournik for taking the time to be one of the committee members of my thesis.

I am grateful for Dr. Fahes who provided me with equipment, tools and her time for the development and completion of this thesis during my graduate studies at the Mewbourne School of Petroleum and Geological Engineering at the University of Oklahoma.

Table of Contents

List of Tables

List of Figures

Abstract

The gas lift system and ESP are used to enhance oil production from a well. The basic principle of gas lift technique is reducing the gravity component of the pressure by injecting gas, thus increasing the oil production from a well. An ESP, on the other hand, boosts the production of fluid after exposing it to great centrifugal forces and rotations inside each pump stage that leads to a change of kinetic energy to potential energy and thus increasing pressure. Both techniques aid in lifting the fluid to surface and improve production. Previous investigations underlined the effect of both systems on three phase flow in vertical pipes but few studied the behavior of emulsion inside these two methods.

In a vertical production tubing, water and oil flow together forming a liquid mixture. Under some circumstances when emulsifying agents are present, the emulsion is formed composed of a dispersed phase in a continuous phase either oil drops in water or water drops in oil emulsion. The viscosity of formed emulsion increases compared to the viscosity of each phase.

In this thesis, the influence of gas injection on water-oil emulsion in a vertical pipe, and the effect of a centrifugal pump on emulsion properties were investigated. The main focus was on the viscosity and pressure gradient changes.

Small scale experiments were conducted in the laboratory. The first phase of the experiment was to build the vertical flow loop and test it with water. The two phase (water-air) flow experiments revealed the compatibility of the system with our needs where gas injection reduced the pressure drop as predicted by correlations.

The second phase of experiments was lifting oil. Further measurements were done on mineral oil to confirm that the centrifugal pump and the gas injection would operate well with a viscous fluid and that we can reduce the gravitational part of the pressure drop.

Finally, the third phase of the experiments included running the emulsion through a centrifugal pump and exposing it to gas injection to investigate the influence on emulsion properties such as viscosity changes and pressure drops. We quantified the impact the centrifugal pump had on the viscosity of the emulsion. The gas lift data suggest that the technique becomes less efficient in the presence of emulsions but has a positive impact by reducing the viscosity and the stability of the emulsion.

Chapter 1. Introduction

1.1 Purpose and Significance of the Study

Artificial list systems are used widely in planning oilfield projects. It is a method to improve the fluid production from a well, which has relatively low reservoir pressure to boost the desired production rate to the surface. Such a concept is essential for developed oilfields, especially the ones in the Middle East.

Using an ESP in a well enhances the crude oil production. In case of water continuous flow, the formation of stable water-oil emulsions is possible and spontaneous. Its stability depends on the fluid flowrate, water volume fraction, droplet size, and physical properties of the fluids. Many useful correlations are published in the literature between the relative viscosity of water-oil emulsions and their water volume content and the phase density of oil. However, there is shortage of experimental data to validate and generalize for most of these correlations (Oliveria and Goncalves, 2005).

The water-oil emulsion formation and its problems in existing artificial lift systems such as an ESP or a gas lift unit have been studied very briefly and few work has been done in this area. The aim of this work is to gather experimental data for the behavior of emulsions in a vertical loop system and investigate the effect of gas injection and centrifugal pump on emulsion viscosity and pressure drops. An added understanding of the impact of emulsions on the ESP system and the ESP role in stabilizing the emulsion is addressed.

Chapter 2. Review of Literature

In this chapter, we present an overview of artificial lift systems, water-oil emulsions, and an analysis of recent literature on the role of emulsion in this system

2.1 Artificial Lift

For any production installation, it is vital to increase the use of natural energy in a reservoir. The reservoir pressure in a naturally flowing well is sufficient to produce the fluid up to the surface. Once the reservoir energy is insufficient to flow the well naturally or the production rate is not satisfactory, it is essential to use any form of artificial lift that is most adequate to the well.

2.1.1 General Description

In an oil well, if it is incapable of producing due to the decrease in the bottom hole pressure or the increase in pressure losses, the well stops flowing naturally and eventually dies. Some of the reasons of upraised issue could be due to the increase in overall fluid density, the decrease in gas production, the increase in water cut, or some mechanical deficiency downhole such as scale.

There are two categories in classifying artificial lift methods;

Pump Category:

- Sucker Rod Pump (SRP)
- Progressive Cavity Pump (PCP)
- Surface Hydraulic Pump
- Electrical Submersible Pump (ESP)

Gas Category:

- Gas Lift System

2.1.2 Artificial Lift Selection

In oilfield development, the optimum artificial lift method should be elected to maximize the field potential. The are several common methods to select the most suitable artificial lift system

2.1.2.1 Selection Based on Depth/Rate

The depth and rate ranges of each artificial lift are summarized in a chart. This chart is helpful for preliminary selection as well as considering the advantages and disadvantages of each method. However, well conditions might indicate another artificial lift method, to better optimum choice. Each well has its unique conditions that require a specific design for precise rate prediction at given depths (Clegg, 2007).

2.1.2.2 Selection Based on Advantages and Disadvantages

The pros and cons for the two main artificial lift methods used in Saudi Arabia are summarized in **Table 2-1**, meanwhile the design consideration for ESP and gas lift are shown in **Table 2-2**. In the selection procedure, these two tables are accompanied with the depth rate charts for better design assortment despite any critical conditions (Clegg, 2007).

Examples of points to consider are reservoir characteristics and location of each well. It is not recommended to choose a method to produce high rates if the well is anticipated to deplete soon. Another example would be having a source of gas available near well site that promotes the selection of gas lift system instead of an ESP (Heinze et. al., 1996).

Table 2-1 Advantages and disadvantages of ESP and Gas Lift system (Clegg, 2007)

ESP		Gas Lift	
Advantage	Disadvantage	Advantage	Disadvantage
Can lift extremely high volumes	Only applicable with electric power	Can handle large volumes of solids with minor problems	Not efficient in lifting small fields or one-well leases
Unobtrusive in urban locations	High voltages (1000 V) are necessary	Handles large volume in high PI wells	Safety problem with high pressure gas
Applicable offshore	Impractical in shallow, low volume wells	Unobtrusive in urban locations	Gas freezing and hydrate problems
Corrosion and scale treatment easy to perform	Expensive to change equipment to match declining well capability	Power source can be remotely located	Difficult to lift emulsions and viscous crude
Simple to operate	Cable causes problems in handling tubulars	Lifting gassy wells is no problem	Lift gas is not always available
Easy to install downhole pressure sensor for telemetering pressure to surface cable	System is depth limited because of cable cost and inability to install enough power downhole	Fairly flexible-convertible from continuous to intermittent to plunger lift as well declines	Some difficulty in analyzing property without engineering supervision
Availability of different sizes	Not easily analyzable unless good engineering know how	Easy to obtain downhole pressure and gradients	Casing must withstand lift pressure
Lifting costs for high volumes generally very low	Gas and solids production are troublesome	Sometimes serviceable with wireline unit	Cannot effectively produce deep wells to abandonment
Crooked holes present no problem	Lack of production rate flexibility	Crooked holes present no problem	
	More downtime when problems are encountered because of the entire unit being downhole	Corrosion is not usually as adverse	
	Casing size limitations	Applicable offshore	

Table 2-2 Design consideration and overall comparison (Clegg, 2007)

Consideration /System	ESP	Gas Lift
Capital cost details	Relatively low capital cost if electric power available. Costs increase as horsepower increases	Well gas lift equipment cost low but compression cost may be high. Central compression system reduces overall cost per well
Downhole Equipment	Requires proper cable in addition to motor, pumps, seals, etc. Good design plus good operating practices essential	Good valve design and spacing essential. Moderate cost for well equipment. Choice of wireline retrievable or conventional valves
Operating Efficiency	Good for high-rate wells but decreases significantly for <1000 BPD. Efficiency can be <40% for low-rate well and 60% in a high-rate	Fair. Increases for wells that require small injection GLRs. Low for wells requiring high GLRs. Typically 20%, but range from 5 to 30%
Flexibility of System	Poor for fixed speed. Requires careful design. Variable speed drive provides better flexibility	Excellent. Gas injection rate varied to change rates. Tubing needs to be sized correctly
Miscellaneous Problems	Requires a highly reliable electric power system. System very sensitive to changes downhole or in fluid properties	A highly reliable compressor with 95+% run time required. Gas must be properly dehydrated to avoid gas freezing
Operating Costs	Varies. If high horsepower, high energy costs result from short run life especially in offshore operation. Repair costs often high	Well costs low. Compression cost varies depending on fuel cost and compressor maintenance
System Reliability	Varies. Excellent for ideal lift cases; poor for problem areas (very sensitive to operating temperatures and electrical malfunctions)	Excellent if compression system properly designed and maintained
Salvage Value	Fair. Some trade-in value. Poor open-market values	Fair. Some market for good used compressors and mandrels/valves
System Total	Fairly simple to design but requires good rate data. System not forgiving.	An adequate volume, high pressure, dry, noncorrosive, and clean gas supply source is needed. Good data needed for valve design and spacing

Table 2-3 Problems and considerations (Clegg, 2007)

Consideration /System	ESP	Gas Lift
Casing Size Limit	Casing size will limit use of large motors and pumps. Avoid 4.5 in casing and smaller. Reduced performance inside 5.5 in casing depending on depth and rate	The use of 4.5 and 5.5 in casing with 2 in nominal tubing normally limits rates to <1000 BPD.for rates >5000 BPD larger (>7") casing and >4.5" tubing needed
Depth Limits	Usually limited to motor horsepower or temperature. Practical depth approximately 10,000 ft. 1000 to 10,000 ft TVD typical; 15,000 TVD maximum	Controlled by system injection pressure and both gas and fluid rate. Typically for 1,000 BPD with 2.5" tubing, a 1,440 psi lift system, and a 1,000 GLR, has an injection depth <10,000 ft; 15,000 ft maximum
Intake Capabilities	Fair if little free gas (i.e., p>250 psi), Poor if $\varphi = 666(Vg/Vl)/p$ >1.0. 5% gas at low pressures can cause problems	Poor. Restricted by the gradient of the gas lifted fluid. Typically moderate rate is limited to approximately 150 psi per 1000 ft of injected depth. Thus, the backpressure on 10,000 ft well may be >1,500 psig
Noise Level	Excellent. Very low noise often preferred in urban areas if production rate high	Low at well but noisy at compressor
Obtrusiveness	Good. Low-profile but requires transformer bank	Good low profile, but must provide for compressor. Safety precautions must be taken for high-pressure gas lines
Prime Mover Flexibility	Fair. Requires a good power source without spikes or interruptions.	Good. Engines, turbines, or motors can be used for compression
Surveillance	Fair. Electrical checks but special equipment needed otherwise	Good excellent. Can be analyzed easily. BHP and production log surveys easily obtained.
Relative Ease of Well Testing	Good. Simple with few problems. High water cut and high-rate wells may require a free water knockout	Fair. Well testing complicated by injection gas volume/rate
Corrosion/Scale Handling Ability	Fair. Batch-treating inhibitor only to intake unless shroud is used	Good. Inhibitor in the injection gas and or batch inhibiting down tubing feasible. Steps must be taken to avoid corrosion in injection gas lines

2.1.2.3 Selection Based on Net Present Value

The lifetime economics of the available artificial lift methods can help in determining the method to be selected. The economics rely on several factors such as the failure rate of the system components, fuel expenses, maintenance expenses, inflation rates, and expected profit from produced oil and gas. The first step to use the NPV as a comparison method is to have a decent knowledge of the associated costs of each technique along with the advantages and disadvantages and any supplementary costs that might be needed. Since energy expenses are used in the NPV analysis, there should be a design for each feasible system before evaluating the economic analysis to better determine the efficiency of a specific installation (Clegg, 2007).

A typical NPV formula is as follows,

$$NPV = \sum_{i=1}^{n} \frac{WI(Q_{HC} * P_{HC} - Cost - Tax)_i}{(1+k)^i} \quad \textbf{(2 - 1)}$$

where:

WI = work interest

Q = oil rate

P = oil price

Cost = all costs, operation (Opex) and capital (Capex)

Tax = governmental taxes

k = depreciation rate of the project (percent)

2.2 Electrical Submersible Pumps

It is an efficient and reliable artificial lift system for lifting moderate to high liquid volume. An ESP consists of the following: a multistage centrifugal pump, a

three-phase induction motor, a seal chamber unit, an intake or gas separator, a power cable, and surface controls. The ESP is normally hanged with production tubing from the wellhead, the pump being on top and the motor below. The power cable is clamped to the tubing and plugs into the top of the motor. There is also an inverted configuration for certain applications.

As the fluid enters the well, it passes the motor and goes inside the pump through the intake. The bypass fluid cools down the motor. Each stage consists of an impeller and a diffuser that add pressure or head to the fluid at a certain rate. As the fluid reaches the top of the pump it gains energy to be lifted to surface and into the separator or flowline.

The downhole components of an ESP displayed in **Figure 2-1** are (Amao, 2014):

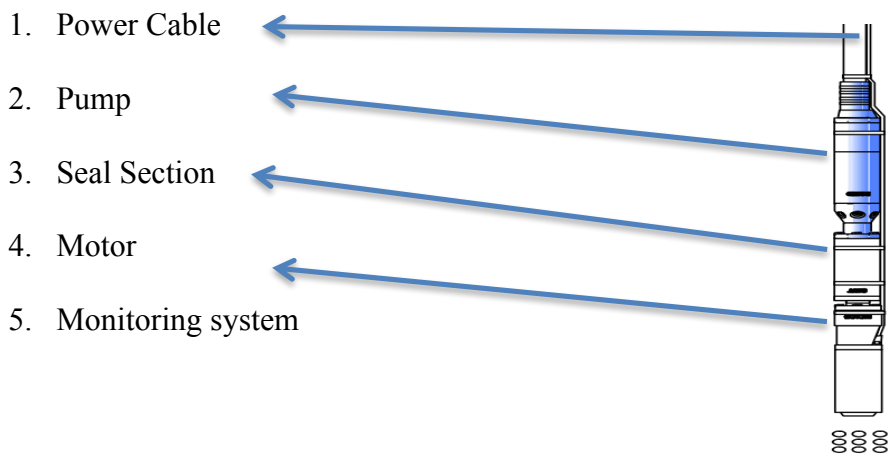

Figure 2-1 Basic ESP configuration (Stanghelle, 2009)

The full ESP system is shown in **Figure 2-2**. Since the focus of the study is not the ESP setup, the surface equipment is not described in details. The surface controller delivers power to the ESP motor and protects the downhole parts. The design of surface controller can differ in complexity providing several options to improve the control

methods, protect and monitor the operations.

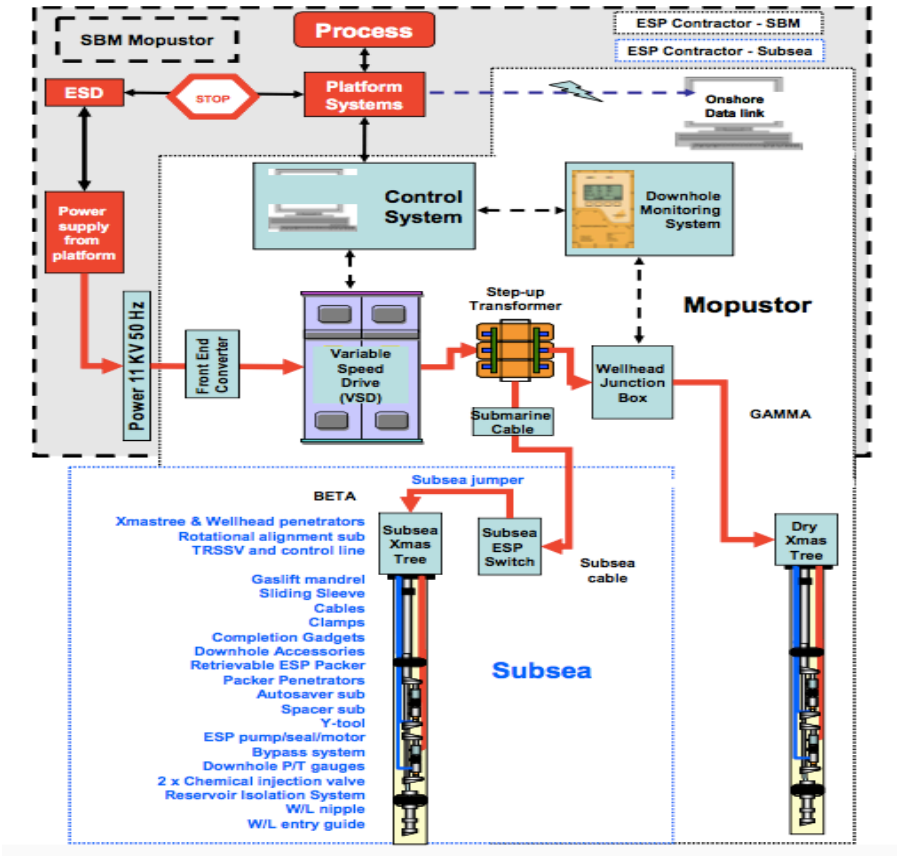

Figure 2-2 ESP surface system (Stanghelle, 2009)

ESP has a wide performance range and is an adaptable lift method. It can lift volumes of fluid ranging from a low of 150 BPD to as much as 150,000 BPD (24 to 24,600 m^3/d). The variable speed controller provides additional flexibility to the pump. ESP can handle high GOR fluids but large volumes of free gas can lock up and terminate the pump. Corrosive fluids can be dealt with by selecting special materials and coatings. The modified designs protect the equipment from hostile effects caused by abrasive particles or sand. We next discuss the various components of the ESP pump system from top down.

2.2.1 Centrifugal Pump

The ESP contains a multistage centrifugal system. **Figure 2-3** illustrates a cross section of a standard design. The centrifugal pump adds energy to the fluid through the centrifugal force and transfers it to pressure to lift it at a desired flow rate from wellbore.

The pump is manufactured with different diameters to optimize the lift and head from several casing sizes (Amao, 2014).

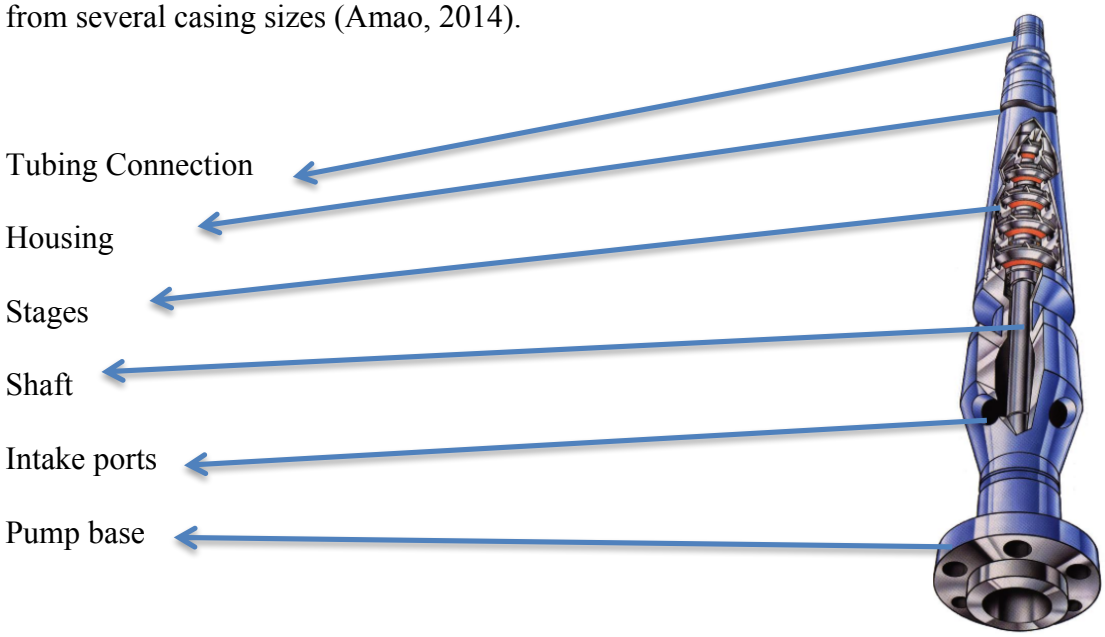

Figure 2-3 The inside of a centrifugal pump (Stanghelle, 2009)

2.2.1.1 Functional features

Starting from bottom, the shaft, seal section and motor are tied with spline coupling. It conveys the rotational movement from the motor to the impellers inside the pump stage. The key, which connects shaft to impellers, transmits the torque load. The diameter of the shaft is reduced as much as possible to overcome the restriction imposed by the pump outside diameter.

Then, the free gas is controlled within an ESP through a downhole mechanical separation part such as separator intakes. This device imparts a centrifugal force upon the entrance of the fluid to separate the lighter and heavier density fluid. The light density fluid goes through annulus while the heavier fluid passes through the first pump stage.

The next part is the stages of the pump that transfer pressure to the fluid. Each stage is composed of a rotating impeller and stationary diffuser. The stages are assembled in series to raise the pressure needed for a desired flow rate. The path of the fluid inside the stages is demonstrated in **Figure 2-4**. As the fluid moves towards the impeller eye area, it gains energy in form of velocity while it is centrifuged radially upward in impeller pathway. This process recurs for the next impeller and diffuser until the fluid crosses all the stages and planned pressure is met. The increase in pressure indicates the total developed head of the pump (TDH).

For the range of flow rates that ESP can function, there are two types of stages; the radial and the mixed-flow stage. The geometry of the radial stage allows the fluid to enter the impeller or diffuser parallel to axis of the shaft whereas it exits perpendicular to the shaft. The second type, the mixed-flow stage, has a geometry that permits the fluid to exit at an angle less than 90° to the shaft. It has higher range of flow rates and is less susceptible to free gas and particles.

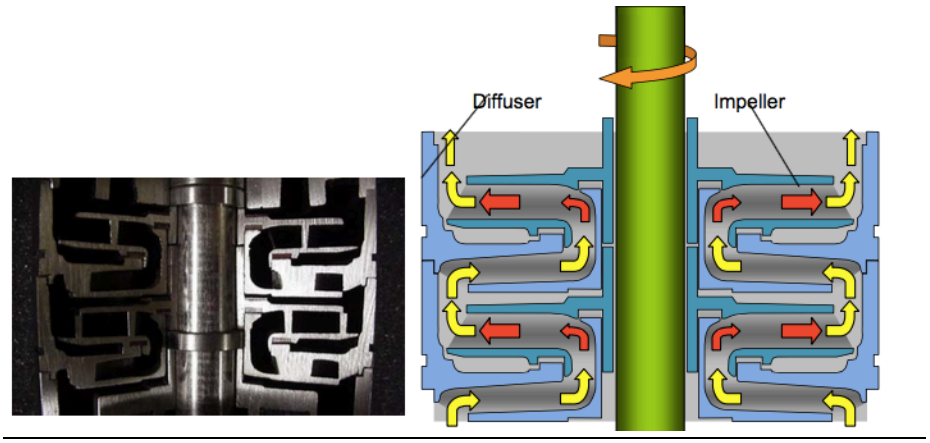

Figure 2-4 Shaft with rotating impellers and stationary diffusers (Stanghelle, 2009)

The main feature in both types is the way they handle the produced axial thrust. Normally, pumps with diameter smaller than 6 in. are built as floater stages. These types permit the impellers to travel axially on the shaft between the stationary diffusers. They operate in a down-thrust position but at high flow rates they switch to up-thrust position. The impellers are manufactured to work in a down-thrust position inside the operating range to sustain the best flow passageway alignment between the impeller and its diffuser for each stage, see **Figure 2-5**.

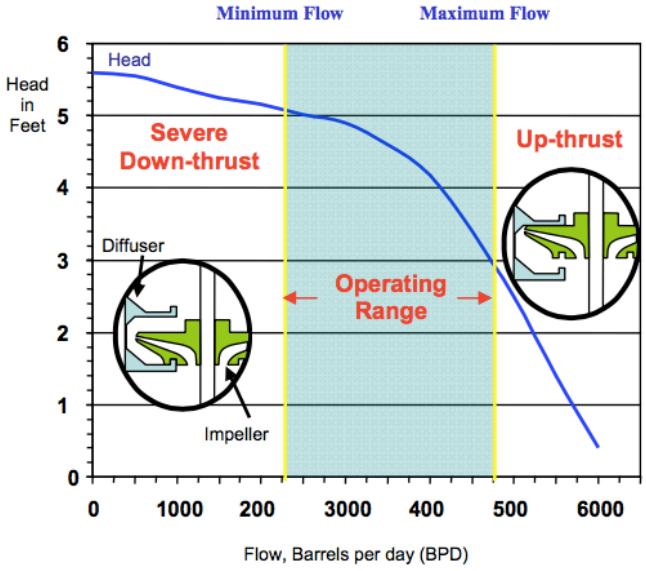

Figure 2-5 ESP operating range (Stanghelle, 2009)

The manufacturers provide the pump performance characteristics for 1 stage, 1.0 S.G of water at 60 – 70 Hz power. Figure 2.6 displays a typical ESP performance curve. The head capacity, pump efficiency and brake horsepower are plotted versus flow rate. The formula for pump efficiency is as follows,

$$\eta_p = \frac{Q * TDH * S.G}{C * BHP}$$

(2 - 2)

The head capacity curve represents the lift measured in feet or meters that can be obtained by single stage. The pump tends to have similar head for all type of fluids because the head is independent of fluid S.G. except for fluids which are very viscous or contain free gas. If the curve is measured in pressure, different specific curve are plotted based on each fluid S.G.

The shaded area in the graph represents the manufacturer's recommended operating area. It is more reliable to work under this range. The left edge is the minimum operating point and the right edge is the maximum operating point. The optimum efficiency point is between these two edges at the peak of the curve. The shape of the head curve along with the thrust characteristics donate the minimum and maximum points. The minimum point is placed where the head curve is still increasing before it is dropping at reasonable down-thrust value. The maximum point position is determined by the impeller stable performance, taking into consideration the thrust value, head produced and adequate efficiency.

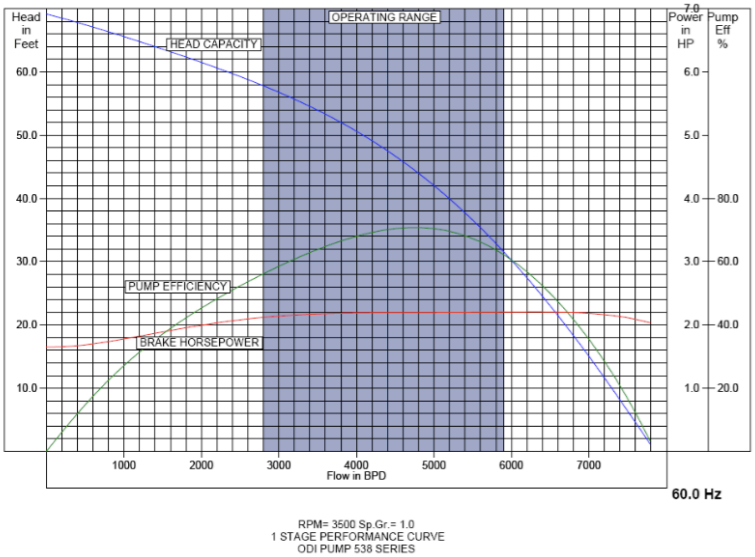

Figure 2-6 Standard pump curve for head, efficiency, and brake horsepower (Stanghelle, 2009)

2.2.2 Seal Chamber Section

The seal section is placed between the top of motor and below the lowest pump part. It is a cluster of seal chambers joined together in series or parallel. The seal chamber section plays a critical role in the operation and run-life of an ESP system. The functions of this seal are as follows:

- It preserves the motor oil from contamination caused by wellbore fluid, see **Figure 2-7**
- It equalizes the pressure between the core of motor and wellbore
- It stands the axial thrust generated by the pump and dispels the heat produced by the thrust bearing.

Figure 2-7 A mechanical seal located at the top of protection chamber to prevent fluid from traveling down the drive shaft (Stanghelle, 2009)

2.2.3 The Motor

The motor is similar to a squirrel cage, dipole, and three-phase induction design. Dipole design is referred to the motor speed of 3,600 rpm at power of 60 Hz. The three-phase power motor operates at voltages that range from 230 to 5,000 V with 12 to 200 amperages. The HP rating of a motor is controlled by its length and diameter. Some motors are built slightly larger in diameter compared to the pump and seal because the power cable does not run along its length.

2.2.4 The Power Cable

The power is transferred to the ESP motor from the surface through the three-phase power cable. It is fastened to the production tubing under the wellhead to the ESP unit because it lacks weight support. It is constructed in a way to uphold downhole severe conditions. The diameter of the cable is designed in small sizes to protect it from mechanical complications and physical and electrical deterioration caused by well

hostile environments. The cable can be designed in either round or flat shape as illustrated in **Figure 2-8** and **Figure 2-9**. Round is considered as the best conductor meanwhile the flat design is used underneath the ESP packer and beside the pump and seal section due to the limited clearance between casing and an ESP.

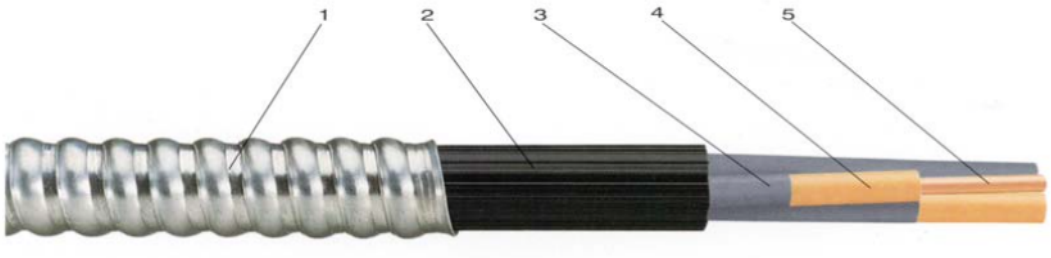

Figure 2-8 Round ESP cable design, 1-Armour, 2-Jacket, 3-Basic insulation, 4-Physical filler, 5-Conductor (Stanghelle, 2009)

Figure 2-9 Flat ESP cable design, 1-Armour, 2-Braid, 3-Barrier layer, 4-Jacket, 5-Conductor/Insulation gas block, 6-Conductor (Stanghelle, 2009)

2.2.5 ESP Run Life

There are several factors that contribute to the run life of an ESP. These factors are described as equipment, operation and operating environment. The reliability model for ESP is categorized into three stages.

Stage 1 Infant mortality: ESP early time failure (fails to start at installation).

Stage 2 In-service failures: Operational issues

Stage 3 Wear out: failures caused by pump wear out

The failure rates are diagnosed and analyzed individually because they are independent of each other. Stage 1 happens in the first two days of operation upon destroying the equipment while running in hole, misconnecting the electrical cable, or leaving external objects in the well.

Stage 2 is independent of time and it is related to the field operation of equipment. Electrical failures are part of stage 2. It occurs when there is an inadequate cooling unit and it is preventable under cautious supervision. The pressure rotation may also affect the pump cable and cause it to crash.

Stage 3 is diagnosed less often compared to the other stages due to a proactive workover schedule for maintenance.

The following is a list of factors that affect the run life of an ESP;

2.2.5.1 Design and Sizing:

Appropriate sizing of an ESP unit is critical in having an extended run life. The equipment size selected should be operated inside the recommended flow range. In order to select the proper size, we must obtain accurate well productivity data. In case of choosing inappropriate size, the ESP will operate outside of the recommended operating range leading the ESP pump to wear out fast and the motor to burn due to overload gas locking.

2.2.5.2 Operating Practice:

Inadequate operating practice causes an ESP to fail. This can happen due to insufficient knowledge in the functionality of the unit or sudden change in operating conditions. Downhole information can yield better ESP performance. Real time

downhole data for pressure and temperature can aid in supporting, protecting and optimizing the operation of ESP.

2.2.5.3 Bottom Hole Temperature (BHT):

Any bottomhole temperature that exceeds 105 ^{o}C is perceived as a high temperature for ESP application. It is essential to check the motor assembly for clearance at high temperatures. Not following these actions could result in reducing the component run life and MTTF (Mean Time to Failure).

2.2.5.4 Free Gas:

The ESP is not designed to pump gas, and as a result, any free gas breaking through or alternating slugs of liquid and gas can cause severe complications. If the velocity of the fluid bypassing the motor decreases, the cooling efficiency drops significantly causing the motor to burn or overheat. In agonizing conditions where the percentage of free gas grows significantly, the pump starts to suffer head loss and swirls no liquid in a situation termed gas locking.

2.2.5.5 Viscosity:

Fluid having relatively high viscosity can create several problems. The pump horsepower specification escalates when the specific gravity of the fluid rises. The pump efficiency and ability to ascend fluid decreases as the viscosity increases. The viscous fluid creates additional frictional pressure losses in the tubing forcing the pump to perform harder. The viscosity of the fluid might change due to the shear force applied by the pump; and it can change upon different water cuts. Tight water-oil emulsions can be generated under specific circumstances.

2.2.5.6 Corrosion:

Corrosion formed due to CO_2 and H_2S can endanger the ESP unit by rapidly eroding electrical connections and seals. Selecting proper materials can eliminate these concerns.

2.2.5.7 Sand Abrasion:

Sand production affects the pump efficiency negatively because it damages the stages. An instant collapse can happen due to pump shaft vibration, which causes mechanical failure to the seal and burns out the motor as a result of fluid transportation. The solution to these subsequent issues is to cast out or lessen sand production. In order to control sand production, a clear understanding of sand mobilization rates is necessary. Selecting the proper material and an abrasion resistant pump design can help in reducing the damage caused by sand to the impellers and pump stages and provide some stabilization to the radial shaft.

2.2.5.8 Deposition:

Asphaltenes, hydrates, scale and paraffin can precipitate in ESPs. These can block pump inflow causing the efficiency to drop and the possibility of burning out the motor.

2.2.5.9 Electrical Failure:

It is possible to have electrical failure either at surface or downhole. The obstacles at the surface including overburden of the transformer or controller can be treated effortlessly more than the ones downhole. When changing out an ESP due to those downhole problems, the power source is disconnected and a workover intervention is done.

2.2.5.10 Old Age:

There will be time where specific components of ESP reach failure point despite an ESP working inside the design envelope and having proper maintenance periodically.

2.2.5.11 Reliability Issues Specific to High Horse Power Units:

There is a great risk when the horsepower is high. A unit with high HP consists of more motor sections making it greater in length than other units. This can create difficulties and mechanical damage of the unit placing it in stage 1 (infant mortality category) of the reliability model. Dogleg severity and deviation limits should be tougher for the longer length units. The pump is run inside an enclosed pod to resist some of the mechanical damage while running in hole. A series of low horsepower pumps are connected to create a higher horsepower pump. The dependency between the series reduces the reliability of the system because the requirement for high power and torque is delivered to one motor then transferred to the others (Meihack, 1997).

2.3 Gas Lift System

The procedure involves injecting gas in the annulus where it exits the annulus to the tubing through a gas lift valve placed inside a mandrel or side pocket. The injected gas helps in reducing the average produced fluid density, which decreases the bottomhole pressure. Accordingly, the restrictions imposed on fluid in the reservoir decrease, resulting in higher production flow rates.

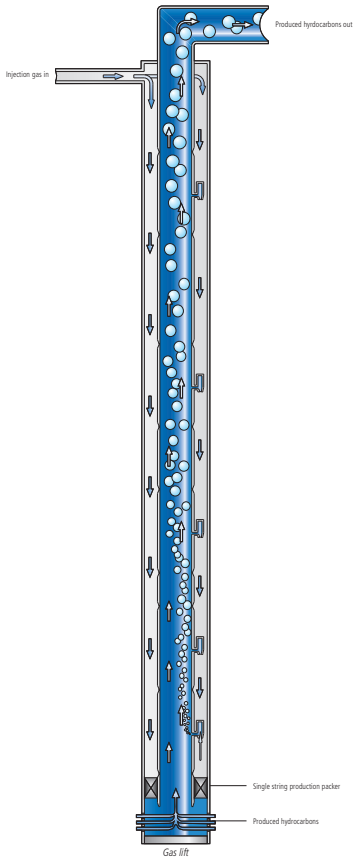

Figure 2-10 Gas Lift System showing the injected gas through the annulus (Baker Huges, 2014)

The flow process in this artificial lift method is similar to a natural flow procedure. The only item needed is a source of gas nearby to be injected. Generally, the separated gas from produced oil in another well is compressed in a gas compressor and pumped in the annulus at a high-pressure. The recovered gas from the produced fluid is then recompressed and re-injected again in the well. The procedure of compressing the gas; however, is costly and power consuming.

There are several types of gas lift systems, a typical continuous flow gas lift similar to the one in **Figure 2-10**, intermittent gas lift, and dual gas lift.

Intermittent gas lift:

The method involves injecting the gas at different intermissions in low producing wells. Prior to injecting a slug of gas, the liquid level should be sufficient at the bottom of the well.

Dual gas lift:

Instead of drilling two wells for independent reservoir sections on a rig, it is possible to have dual tubing completions in the same well. The gas lift unit is supplied in a mutual casing and injected through different gas lift valves. The alternative technique is to inject the gas in one string and produce from the second (Baker Huges, 2014).

2.3.1 The Unloading Process

After completing a well or work over job, the fluid column in the well is close to the surface. The gas lift pressure needed to unload the well to target gas injection depth is insufficient. This is due to the static column of fluid in the well at the desired injection depth being larger than the available gas pressure at injection point. To serve this purpose, a sequence of unloading valves are set in the well to unload the well until it reaches the desired depth of injection using the accessible gas injection pressure. The process is summarized in **Figure 2-11**.

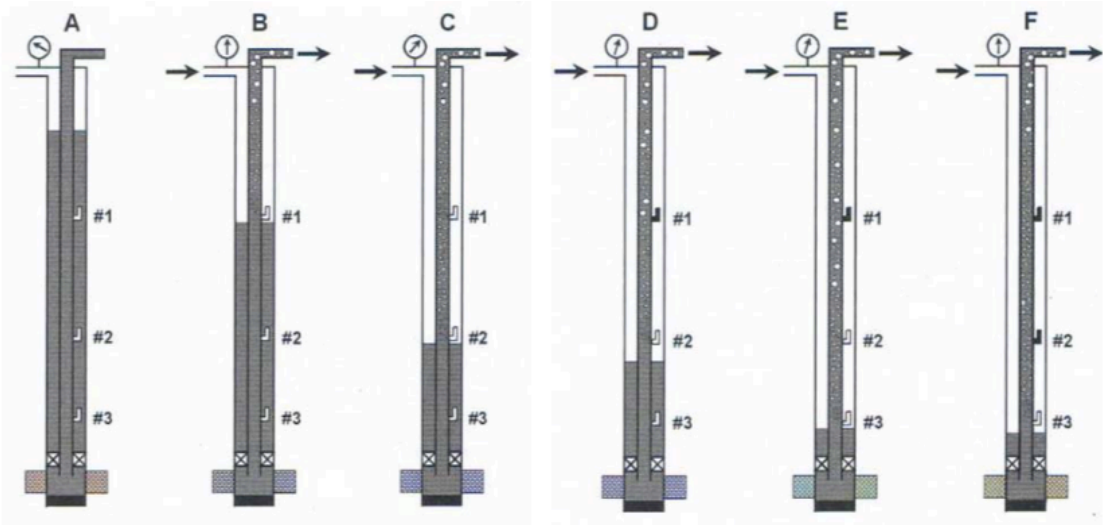

Figure 2-11 The unloading process (Takacs, 2005)

The well illustrated in the figure has three gas lift valves. The two on the top are called unloading valves and the one in the bottom called operating valve. As soon as the gas arrives to the top unloading valve, it is injected inside the tubing (**Figure 2-11** part, B). The bubbles of gas entering the liquid column in the tubing decrease the static pressure at the valve depth to stabilize the low GLR. The next two valves are similarly opened and the liquid level in the annulus keeps dropping.

The most critical point is when the liquid column reaches the next unloading valve in the annulus and the gas is injected through the valve. That is because both unloading valves are injecting gas at the same time as shown in **Figure 2-11** section C. The top valve should be closed to transfer the injection point to the operating valve keeping a single gas injection point. In designing and installing the unloading valves, a proper selection should be made to ensure the top valve closes just after the next lower valve begins injecting gas, **Figure 2-11** part D. As the center valve continues to inject gas, the pressure inside the tubing at the depth of injection decreases along with the liquid level in the annulus. The fluid level in the annulus is going to be below the lowest

valve if a proper unloading string was selected. The gas is injected as soon as it reaches the operating valve and the middle valve is closed (**Figure 2-11** part F). The objective of the unloading process is accomplished and only the operating valve then injects the gas (Takacs, 2005).

2.3.2 Gas Lift Performance Curve

Unloading Valves: The widely used type of unloading gas lift valve is the injection pressure operated valve (IPO). Some of the other types are the production pressure operated valves, balanced bellows valves, balanced flexible sleeve valves and pilot valves.

A typical IPO valve has a nitrogen pre-charge chamber and a flexible bellows assembly that delivers the closing force of the valve. The stem axial position governs the closing or opening force of the valve during the injection process. While injecting gas, the pressure surpasses the closing force applied by the bellows helping the stem to elevate leading the gas to pass through the valve. A sketch of the unloading valve is illustrated in Figure 2-12. The conditions of opening and closing the valve can be seen in the force balance for the valve stem. When the valve is closed, the nitrogen dome pressure, P_d, works on the zone of the bellows, A_d, and gives sufficient force to hold the stem against the port. The remaining forces keep the valve open, such as the largest force which is exerted from the injection pressure P_i. The smallest force is exerted due to the production pressure, P_p, that works on the port area, A_p, of the stem tip. The opening of the valve happens when the sum of the opening forces surpasses the closing force.

$$P_i(A_d - A_p) + P_p A_p > P_d A_d$$

(2 - 3)

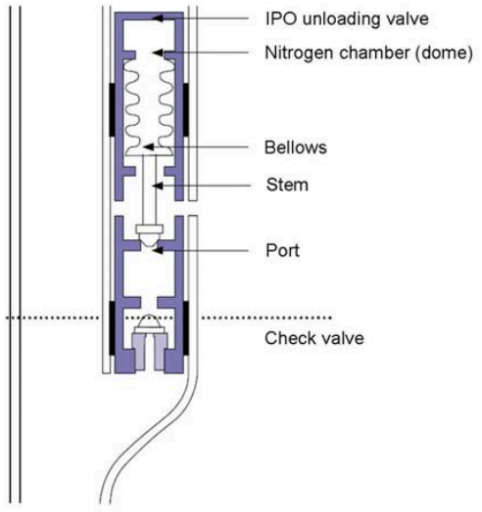

Figure 2-12 Conventional unloading valve (Sclumberger, 2006)

When the forces are in equilibrium, the injection pressure necessary at valve depth to open the valve becomes:

$$P_i = \frac{P_d A_d}{A_d - A_p} - P_p A_p / (A_d - A_p)$$

(2 - 4)

From the equation, it is clear that opening the valve depends on the injection pressure and production pressure. Keeping a constant production pressure, the valve will open only when the injection pressure exceeds the calculated value. **Figure 2-13** shows a graphical demonstration of the valve's functional principle. In the zone between the opening and closing line in the triangle, the state of the valve depends on its prior state. In case of water cut variation, the system is flexible and designed to adapt to such changes. The drawback of this design of valve is that the maximum depth of injection is decreased with every use of unloading valve due to the casing pressure reduction while closing the unloading valve.

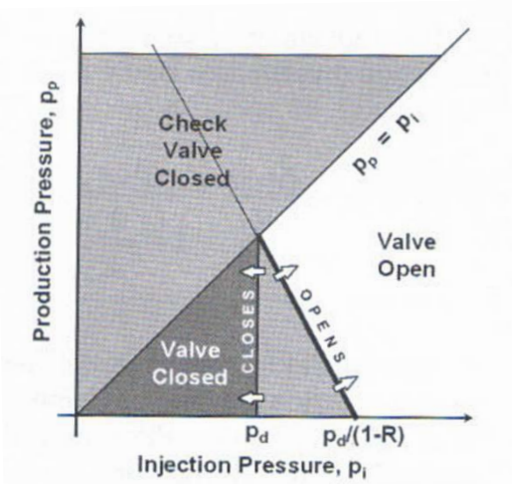

Figure 2-13 Opening and closing performance of an unbalanced IPO gas lift valve (Takacs, 2005)

Operating Valves: The bottommost valve is called the operating valve, or orifice valve. If the gas lift system is continuous, it is better to use the "Nozzle-Venturi valve" instead of the old "square-edged orifice" because it delivers more constant gas rate.

The gas rate increases through the valve in a conventional square edge orifice as the differential pressure along the valve increases gradually until it reaches the critical flow at a critical pressure ratio of 0.55. After reaching the critical flow, any further increase in the differential pressure won't boost the gas rate. Most of the continuous gas lift system works under the subcritical zone which indicate that gas injection range changes with the pressure oscillations at valve depth. The injected gas rate will drop when the tubing pressure at valve depth increases and vice versa. The basic principle of steady state where gas is injected when it is needed contradicts with this behavior. Consequently, it is not recommended to use the square edge orifice valve because of instability challenges. The sizing of the orifice or the throat depends on the injected gas rate necessary to attain critical flow. Installing a large orifice size can cause a drop in the percentage of critical flow. One way to avoid problems accompanying the sub

critical flow and instability is to use the converging-diverging venturi nozzle shown in **Figure 2-14** instead of the square edge orifice size to eliminate the problem and obtain the critical flow at lower differential pressure ratio. **Figure 2-15** shows that a venturi valve will reach critical flow at roughly 0.9 in differential pressure ratio. It indicates that the gas injection rate will remain stable and independent of tubing pressure variations. But this valve is less flexible for any future changes. To avoid backflow within the tubing casing annulus, standard reverse flow check valves are used (Takacs, 2005).

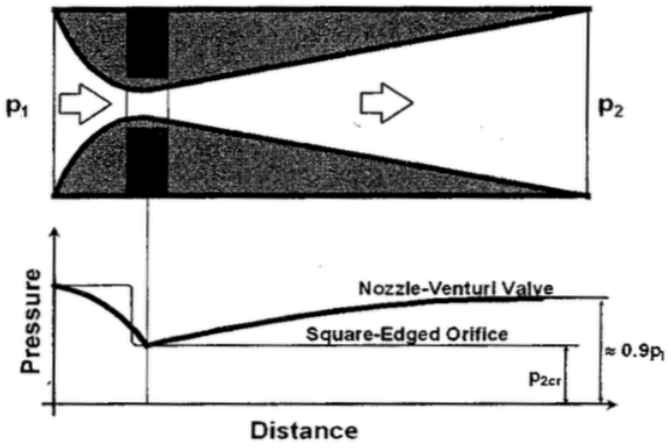

Figure 2-14 Cross section of venturi valve and pressure profile for square edge orifice (Takacs, 2005)

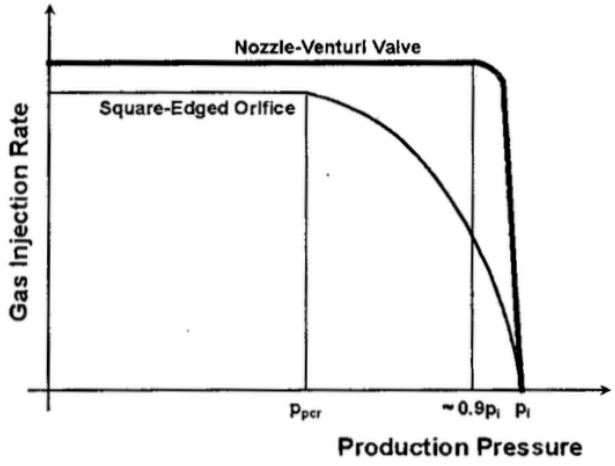

Figure 2-15 Gas passage characteristics comparison (Takacs, 2005)

2.3.3 Gas Lift Completion Procedure

A sidepocket mandrel is built in the tubing where it has a gas lift valve or a chemical injection valve. The gas lift valve is either installed already in the mandrel or installed and placed inside the mandrel by the wireline tool. Instead of installing a valve that might not be needed, a dummy valve is fitted inside the sidepocket mandrel to isolates the tubing from the annulus. A slickline unit is used to assemble or disassemble the gas lift valve but if the well is deviated above 65 degrees, an electric wireline in addition to a well tractor is used instead. In any of the cases, a kickover-tool (KOT) is run in the well (**Figure 2-16**) (Schlumberger, 2012).

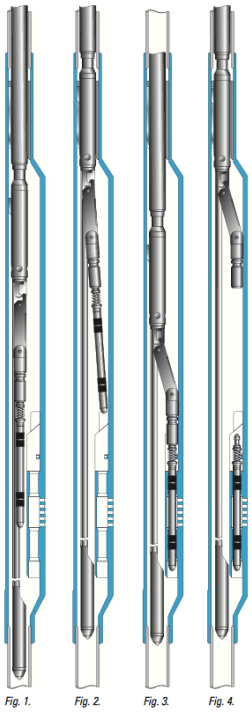

Figure 2-16 Installing a valve using KOT (Schlumberger, 2012)

2.4 Crude Oil Emulsion and Demulsification

In this section, we explore water-oil emulsion as experienced by petroleum engineers.

2.4.1 Background of Emulsion Formation

Emulsions are well-known in most of the petroleum production and processing systems, it can be encountered in the near wellbore zone, wellheads, surface pipelines and crude facilities as seen in **Figure 2-17** (Kokal, 2005).

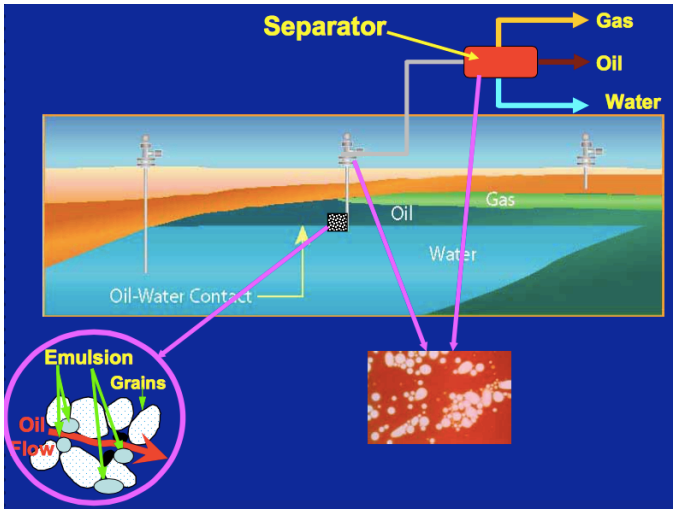

Figure 2-17 Formation of emulsion in the petroleum production System (Kokal, 2008)

One can define emulsion as a firm dispersion of liquid within a different liquid that has restricted miscibility. Its stability is deliberated by the existence of agents at the interfaces postponing the natural tendency of the liquids to discrete. These agents are called surfactants or finely divided solids; they are either polar or non-polar molecules in their structure. The dispersed phase contained in an emulsion has spherical drop shape (Peña, 2004). Emulsification is the term used to describe the process of forming an emulsion. It can occur at high turbulence regions within the petroleum system that develop shearing forces. The deformation of liquid-liquid dispersion due to continuously exerting more stresses is shown in **Figure 2-18** (Kokal, 2005).

The spontaneous emulsification can happen either when the phases are in contact, by chemical reactions (Nishimi, 2001), or by nucleation of a phase into another when the temperature decreases. During the oil production, the produced water experiences a great amount of shearing. Factors that contribute in producing emulsions are agitation effect, heat, pressure, and surface active compounds contained in the crude oil. There are numerous available kinds of compounds in the crude oil varying from pure hydrocarbon to complicated hetero-atomic polycyclics summarized in **Figure 2-19** (Abdel-Raouf, 2012). The amount of water contained while producing oil depends on the content of coincident water and oil present.

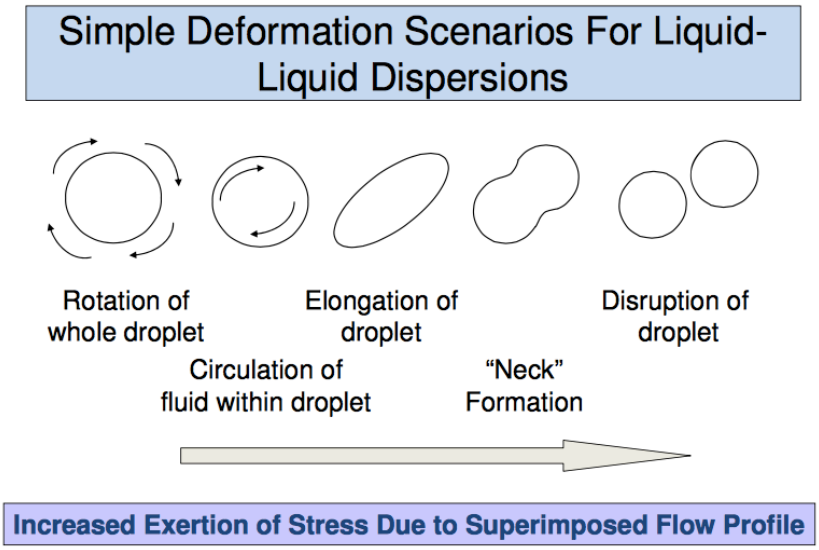

Figure 2-18 Deformation phases for liquid-liquid dispersion (Weiss, 2008)

Historically oil production has been mainly derived from sandstone formations. These formations comprise of a combination of silicon and oxygen that is partially charged, anionic crystallites. The crystallites attract water, which is often available nearby. The close association happens due to the occurrence of hydrogen bonding where the positive charge of hydrogen in water reacts with the partially negative charge

of oxygen in silica (Si_nO_{2n}). The connections cause a layer of water to be formed around the crystallites. This referred to as connate water, which manages to stay close to the silica surface and remain in equilibrium with the free water present in the rock. When the reservoir is produced, the equilibrium condition is agitated and the fluids start to flow.

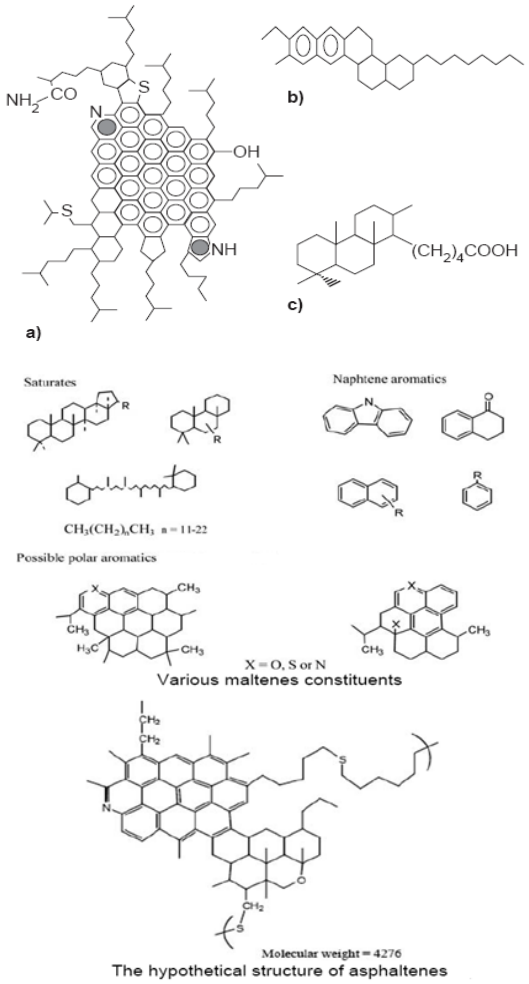

Figure 2-19 Examples of molecules present in crude oil. a-Asphaltenes, b- Resins, c- naphtenic acids (Abdel-Raouf, 2012)

This results in higher shearing forces associated with the change in equilibrium conditions for free-water and its partial pressure in oil phase causing the formation of emulsion. Phase separation is controlled by the thermodynamics; when both the water

and oil form continuous separate phases, the interfacial zone and the free energy of dispersion is decreased. Therefore, the emulsion characteristics such as drop size distribution, mean drop size and additional properties change with time. Thus, the stability of an emulsion can be defined as the capability of the dispersion to maintain its properties within a period of time (Peña, 2004).

2.4.1.1 Conditions for Emulsification

The conditions that need to be present in order to create emulsions are as following:

- There must be a contrast in solubility between the continuous phase and emulsified phase.
- There must be intermediate agents with partial solubility in each phase
- There must be appropriate energy sources to shear the phases.

The first condition demands that the phases needed to emulsify has wide separations in chemical composition which control the solubility. As a consequence to this requirement, another condition is the physical state where both can exist as liquid under the dominant pressure and temperature conditions. The hydrocarbon oil and water satisfy these conditions in the reservoir. The second condition can be satisfied in the presence of emulsifying agents helping in partial solubility. These agents possess compounds with functional groups and they exhibit bipolarity to the intermediate molecules (Schubert, 1992). The last criterion is governed by regions with high pressure drops and turbulence flow for the formation of emulsions. **Figure 2-17** illustrates the possible areas in the petroleum production system exerting high shear on the flowing fluid mixture. The intense mixing conditions at the pressure gradient that the crude oil

experiences as it is transported through chokes and wellhead valves create new water-oil interfaces. As the shearing force acting on the oil-water mixture increases (turbulent flow), the size of water droplets decreases establishing more stable emulsion (Johannes, 2012).

2.4.2 Chemistry and Stabilizing Properties of Emulsifiers

Emulsifiers are active substances that are present in crude oil or added to the crude similar to other production chemicals or surfactant flooding (Becker, 1997). The quantity and quality of the used emulsifier affect the stability and quality of the formed emulsion. The emulsifier exhibits solubility affinity towards one of the liquid phases. Therefore, it accumulates at the interface. Naphthoic acid is an example of an emulsifier, as can be seen in **Figure 2-20** for the effect of the acid on a water droplet dispersed in oil.

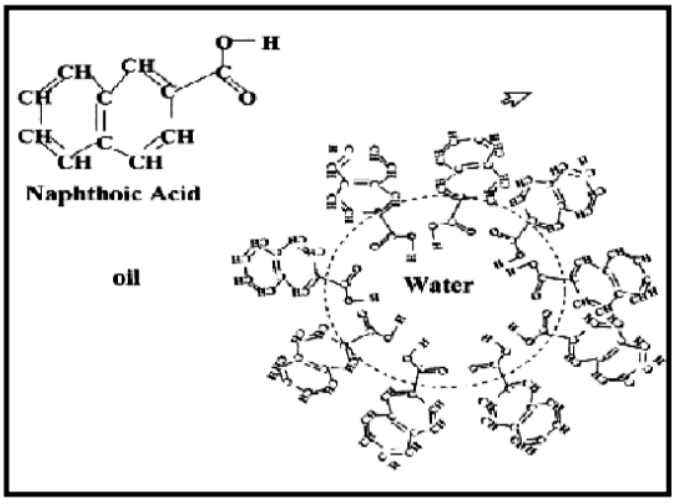

Figure 2-20 Naphthoic acid effect on a water droplet in oil (Becker, 1997)

At equilibrium, the bipolar molecules are coordinated with their nonpolar alkyl (C_nH_{2n+2}) cluster spreading to the non-polar oil phase, and their polar groups in the polar

water phase. This allocation exhibits a stability domain that is preferred by group interactions and fixed conditions such as pressure and temperature. As the continuous phase drains between two dispersed droplets, they stretch and surface tension decreases with increase in emulsifier concentration. Stability is maintained by transport of emulsifiers into the stretched film, lowering surface tension and reducing oil drainage. This process is shown in **Figure 2-21**, a diagram of two water droplets hindered from merging upon the existence of emulsifiers (Becker, 1997) & (Opawale, 2009).

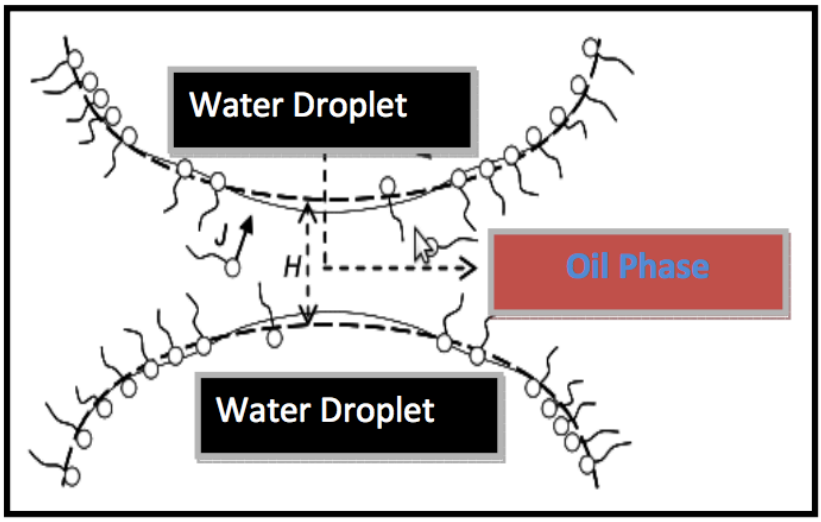

Figure 2-21 Effect of emulsifiers on two dispersed water droplets (Opawale, 2009)

The emulsifying process can be anticipated as following (Carins et al.,1996) & (Singh and Pandey, 1991):

- It reduces the interfacial tension between water droplets, therefore stimulating the formation of smaller water droplets to enhance the stability of emulsions.
- It creates a thin coating that surrounds the droplets and prevents them from colliding and coalescing into bigger droplets thus endorses the stability of formed emulsion.

- The aligned polar molecules in the emulsifier arrange themselves in a proper pattern to generate electric charges on the surface of the droplets increasing the repulsion forces between them and thus reducing the separation of oil and water.

Moreover, there are four types of emulsifiers that stabilize the interfacial tension between oil and water phases. These are:

- Anionic emulsifiers, in which the water soluble group is positive
- Cationic emulsifiers, in which the water soluble group is negative
- Nonionic emulsifiers, in which the water soluble group remains uncharged
- Amphoteric emulsifiers, in which the water soluble groups are both charged positively and negatively.

A schematic graph demonstrating the previous description is shown in **Figure 2-22**. In the petroleum industry, classic examples of emulsifiers involve resins, asphaltene, metal porphyrin complexes and fatty carboxylic acids. All these emulsifiers belong to the higher boiling polar fraction group of crude oil. Examples of inorganic emulsifiers are silts, reservoir fines, scale deposits etc (Schubert, 1992).

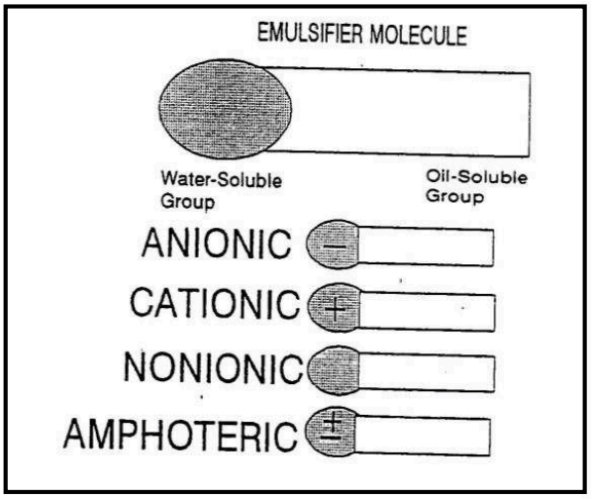

Figure 2-22 Types of emulsifiers (Schubert, 1992)

2.4.3 Morphology of Emulsifiers

Categorizing the type of emulsion can be done using various standards. An emulsion is two immiscible liquids, such as water and oil, one of which is described as the dispersed phase. The continuous phase is denoted as the external phase and the dispersed phase as the internal phase. Considering any liquid as the dispersed phase, we can acquire different emulsion physical characteristics (Schramm, 1992). The main emulsion kinds are identified below:

- Oil-in water (O/W) for oil droplets dispersed in water
- Water-in-oil (W/O) for water droplets dispersed in oil
- Oil-in-water-in-oil (O/W/O) and
- Water-in-oil-in-water (W/O/W).

The last two cases are known when the dispersed droplets themselves include even smaller dispersed droplets of the external phase. The oil dispersed in water dispersed in oil type (O/W/O) and water dispersed in oil dispersed in water (W/O/W) happen as multiple emulsions. The morphology is the basic method in characterizing an emulsion and there are some qualitative processes that can be used as well in classifying emulsion type. This qualitative method relies on physical properties observation such as prevailing polarity in the continuous phase (Peña, 2004).

A simple way in differentiating between elementary and multiple emulsions is by observing whether the external phase is miscible or not when connecting a drop of emulsion with water or oil. But, this technique is not very accurate and precise in distinguishing between them. Another method is the electrical conductivity measurement which is utilized to define the type of emulsion. if the aqueous phase is

continuous, the conductivity of emulsion is great whereas it is low if the continuous phase is oil (Becher, 2001). We can use the optical microscopy as well to discriminate between simple and multiple emulsions due to the noticeable distinction between water and oil phase underneath the microscopy (Peña, 2004).

2.4.3.1 External and Internal Phase of an Emulsion

Determining the type of emulsion depends on phase volume ratios and other factors as explained by Sunil Kokal (2008). Emulsifiers contain both a hydrophilic (water-loving, or polar) head group and a hydrophobic (oil-loving, or nonpolar) tail. Therefore, emulsifiers are attracted to both polar and nonpolar compounds. When added to an O/W emulsion, emulsifiers surround the oil droplet with their nonpolar tails extending into the oil, and their polar head groups facing the water. For a W/O emulsion, the emulsifier's orientation is reversed: nonpolar tails extend outward into the oil phase, while polar head groups point into the water droplet (**Figure 2-21**). This phenomenon is illustrated in **Figure 2-23** and called the hydrophile-lipophile balance (HLB).

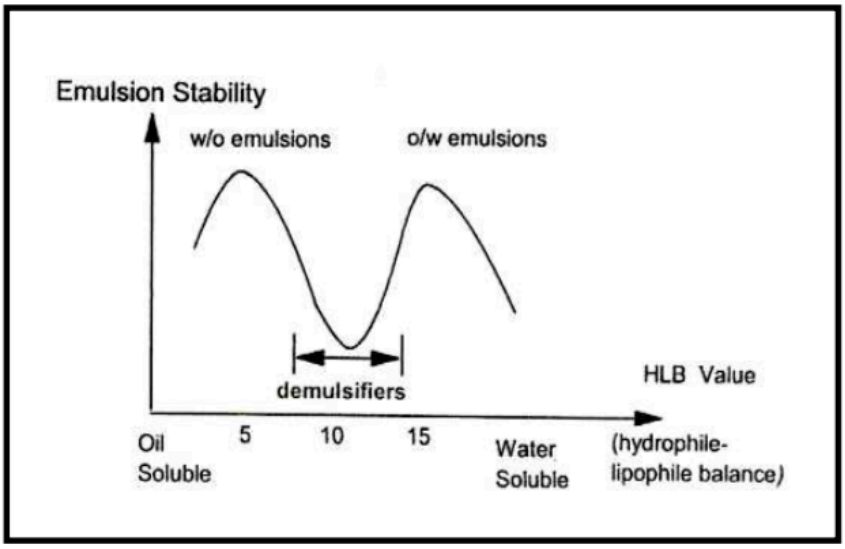

Figure 2-23 Hydrophilic-Lypophylic Balance, HLB (Becher, 2001)

The HLB of the surfactant is used to measure the degree of solubility of the water phase or the oil phase. The surface dynamic molecules having parallel structure (homologous) exhibit the most stability consistently between w/o and o/w emulsifiers. Among these two, there is a stability limit where neither hydrophilic nor hydrophobic groups dictate the interfacial zone. HLB can be found by calculating different regions value of the surfactant molecules. This HLB value is helpful in predicting the surfactant properties of a molecule (Griffin, 1949):

- A value from 0 to 3 indicates an anti-foaming agent
- A value from 4 to 6 indicates a W/O emulsifier
- A value from 7 to 9 indicates a wetting agent
- A value from 8 to 18 indicates an O/W emulsifier
- A value from 13 to 15 is typical detergents

The emulsion kind is controlled by the type the emulsifying agent more than the methodology of forming the emulsion or the comparative amounts of oil or water that

exist (Schubert, 1992). The continuous phase is determined when the emulsifier is more soluble in it. In O/W emulsions, the emulsifying agents tend to be soluble in water more than in oil (High HLB surfactants). Meanwhile in W/O emulsions, the emulsifying agents tend to be soluble in oil more than in water (Low HLB surfactants) (Shaw, 1992).

2.4.3.2 Phase Inversion in Emulsion

The alteration of dispersed and continuous phases of an emulsion from O/W to W/O emulsion and vice versa is called phase inversion. It has two types: transitional and catastrophic inversions. These types are stimulated by varying factors such as temperature or salinity which influence the affinity of surfactants with respect to the two phases. Altering the HLP of an emulsion using the nature and concentration of emulsifying agents can cause inversion. Raising the volume fraction of the dispersed phase prompts the catastrophic inversion. It happens when the internal volume fraction surpasses some specific value. Above this limit, droplets are condensed against each other and the interface is dissolved leading the emulsion to embrace a foam-like configuration (Peña, 2004). A wide study on oil-water flow in horizontal pipes has been conducted for different viscosity values by Arirachakaran et al (1989). In this study, the morphology of emulsion was explained as a function of water cut. Also, increasing the water fraction without the addition of surfactant to the emulsion and maintaining it at constant shear and temperature can produce inversion.

2.4.4 Macroscopic Physical Behavior of Emulsion

One of the essential properties of emulsions is their rheology. It is described as the study of deformation and flow of substances under the effect of applied shear stress.

2.4.4.1 *Emulsion Behavior under Shear Stress*

Due to the emulsion's composition, average droplet's size and the separate viscosities of its phases, it tends to be complex under shear conditions. An emulsion can be Newtonian or non-Newtonian based on its composition (Becker, 1997). There are several factors that influence the shear viscosity of an emulsion such as the viscosity of the continuous phase, the dispersed phase content (φ), the viscosity of dispersed phase, shear rate, temperature, mean size and size distribution of droplets. If the concentration of dispersed phase is low to moderate, emulsions normally show Newtonian rheological behavior. In contrast, if the concentration is high, emulsions act as shear-thinning fluids or thixotropic. There are two reasons for emulsion to behave dilatant or thixotropic, one is the concentration of bipolar emulsifiers at the interface and the other is the equilibrium vapor pressure of the dispersed phase. A velocity profile graph of common fluids and materials is shown in **Figure 2-24** (Schramm, 1992).

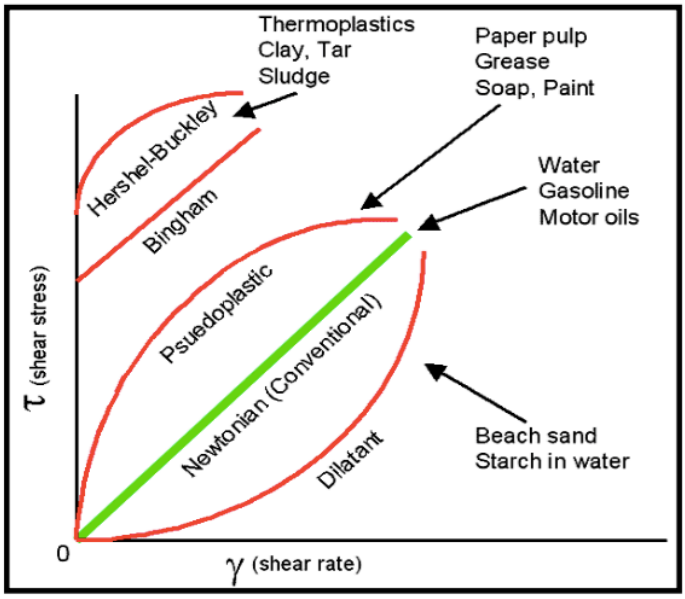

Figure 2-24 Shear stress versus shear rate for different fluids (Schramm, 1992)

2.4.4.2 Emulsion Viscosity Models

The emulsion viscosity is directly proportional to the phase viscosity (μ_c). The term that is used widely in the literature in viscosity correlation equations is relative viscosity (μ_r) where:

$$\mu_r = \frac{\mu}{\mu_c}$$

(2 - 5)

Taylor (1932) developed an early study from hydrodynamic concerns for suspensions of hard spheres, and highlighted the effect of both phases on the viscosity of emulsion with low concentration of dispersed spherical droplets:

$$\mu_r = 1 + \left[0.25\left(\frac{K + 0.4}{K + 1}\right)\right]\varphi$$

(2 - 6)

Where K, is the ratio of the viscosity of the dispersed phase to the continuous phase.

$$K = \frac{\mu_{\square}}{\mu_c}$$

(2 - 7)

As mentioned before, emulsions normally exhibit non-Newtonian behavior (shear-thinning fluids) at high dispersed phase content. There is a need for an empirical methodology to associate the viscosity data. The modified equation of Pal and Rhodes (1989) can be applied:

$$\mu_r = \frac{\eta}{\mu_c} = \left[1 + \frac{\left(\frac{\varphi}{\varphi^*}\right)}{1.187 - \left(\frac{\varphi}{\varphi^*}\right)}\right]^{2.49}$$

(2 - 8)

the dispersed phase concentration φ^*, at which the relative viscosity, η_r = 100, is found experimentally. This equation can be used for both Newtonian and non-Newtonian emulsions.

2.4.4.3 Temperature Effects on Emulsions

Temperature effect is critical since the partial pressures of the internal phase solvent changes upon the temperature alteration. The emulsion preserves a continuous equilibrium movement of internal phase solvent within emulsion mixture at constant pressure and temperature. The equilibrium point transfers when the temperature increases, and a rapid swapping happens. When the temperature increases more dramatically, the molecules gain adequate thermal energy that leads the internal phase to deplete into a solvent due to the increase in the drop collisions frequency. In the meantime, the external phase is depleted into some solvent and the overall stability of the system is controlled by the differential rate of solvent loss between the two phases.

Temperature can influence the physical properties of oil, water, interfacial surface, and surfactant solubilites in the oil and water phases. As a result, the stability of emulsion is affected. Jones et al. (1978) showed that increasing the temperature causes a gradual destabilization of the crude oil/water interfacial films. The most critical effect of temperature will be on the viscosity of emulsions where it decreases when the temperature increases. The reduction in viscosity is mainly controlled by the decreases in oil phase viscosity (Jones et al., 1978).

2.4.4.4 Gravitational Effects on Emulsions

When only the effect of temperature is on emulsions considered, it can cause a tighter (smaller) emulsions or solvent depleted systems. However, gravitational effects

on emulsion are studied as well in this discussion using Stoke's law. This law is important to understand how emulsions behave. The equation of Stoke's law is shown below:

$$V = \frac{2gr^2(\rho_1 - \rho_2)}{9\mu_c} \qquad \textbf{(2 - 9)}$$

where:

V = terminal or settling velocity

r = the radius of the sphere

ρ_1 = density of sphere

ρ_2 = density of medium

μ_c = viscosity of the continuous phase

Joining the effects of temperature and Stroke's law explains the behavior of an emulsion system. Increasing the temperature, increase the sizes of the solvent reservoirs (saturated with oil) and reduce the emulsion sizes. The reservoir is less dense compared to the emulsion since the reservoir is pure solvent and emulsion is a mixture of solute and solvent. Therefore, the ratio of phase density is less. And accordingly, it is anticipated that the difference in densities which is directly proportional to settling velocity would increase. Thus, the effects of gravity and temperature as well as the dynamics of diffusion have great influence on the method of emulsion formation.

The effect of temperature on viscosity has been examined in the past. The behavior of viscosity with temperature is expressed in the following equation:

$$\mu_c = Ae^{\frac{\Delta E}{RT}} \qquad \textbf{(2 - 10)}$$

where:

A = constant

ΔE = change in activation energy

R = Ideal gas constant

T = Temperature of fluid

From the equation it is clear that when the temperature increases, the viscosity drops significantly which causes the settling velocity in Stroke's law to increase.

2.4.5 Emulsion Stability

Emulsions tend to be unstable under normal conditions; it splits into two different phases or layers over a period of time because of the high interfacial area and total surface energy of the system. This indicates that emulsion characteristics will shift with time such as droplet size distribution, mean droplet size and other physical properties.

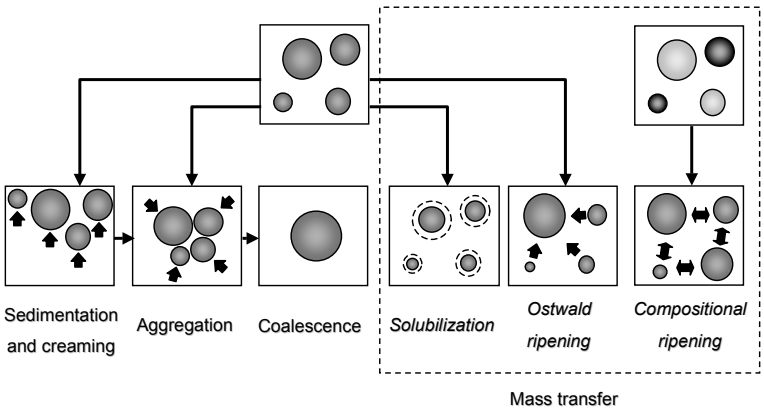

Figure 2-25 Destabilization mechanisms of emulsion (Peña, 2004)

Figure 2-25 shows the destabilization mechanisms of emulsion. Different emulsion separation processes can be recognized. Some of these instability mechanisms cause phase splitting in emulsions such as Sedimentation and Creaming, Aggregation and

Coalescence. Mass transfer processes like Ostwald or Compositional ripening can happen in emulsions in additional to the physical instability. The definition of each physical breakdown method is summarized below (Peña et al., 2006) and (Weiss et al., 2000):

2.4.5.1 Sedimentation and Creaming

The creaming process opposes the sedimentation that happens due to density contrast between two liquid phases. If the particles are transferred in the gravity direction ($\Delta\rho > 0$) then it is called sedimentation otherwise the process is referred to as creaming ($\Delta\rho < 0$). The sedimentation process applicable mostly for W/O emulsions and solid dispersions while creaming applies for O/W emulsions and bubbles dispersed in liquids. In both processes, shaking the emulsions will re-disperse effortlessly. The existence of density contrast between the dispersed and continues phases assists the dispersed droplets in experiencing vertical force under the gravitational field. The fractional drag force opposes this gravitational force. The resultant creaming or sedimentation rate for individual droplet can be determined using Stokes law mentioned earlier (Walstra, 1990).

Nevertheless, this law has several restrictions and is applied only for non-interacting spherical droplets at less concentration with single disperse droplet size distribution. It fulfils the very dilute dispersions and presumes no flow in-between drops (Walstra, 1990). A developed empirical formula is considered for the effect of dispersed phase volume fraction. If the volume fraction of dispersed phase is major ($\varphi > 0.01$), a hindered sedimentation occurs. In general, the effect of φ is to reduce the sedimentation

rate because of the hydrodynamic interactions within droplets. This is expressed by Richardson and Zaki (1954) in the following relationship:

$$\frac{V_{eff}}{V_s} = (1 - \varphi)^{n}$$

(2 - 11)

Where V_{eff} is the effective terminal sedimentation velocity; n is an empirical constant ranges between (6.5 and 8.6).

2.4.5.2 Aggregation

It happens when the droplets are very close to each other and generate an amassment. This process has additional terminology such as coagulation or flocculation. This common term is used to describe emulsion interaction under the DLVO theory written by Derjaguin, Landau (1998) and Verwey and Overbeek (1948) based on the long rage London- van der Waals forces and repulsive electrostatic forces between two close spherical particles.

Hamaker (1997) developed an expression for the London van der Waals attraction for two spherical particles through integrating the interaction energy dU_A over the total volumes of both particles to get U_A. On the other hand, the electrostatic interaction energy U_E for two close spheres showing electrical double layers is not analytically resolvable, instead only an approximation term has been developed. The total interaction energy U is given by the summation of U_A the attraction and U_E repulsion energy. A typical U profile is developed consequently in **Figure 2-26** (Miller and Neogi, 1985) & (Hiemenz, 1986).

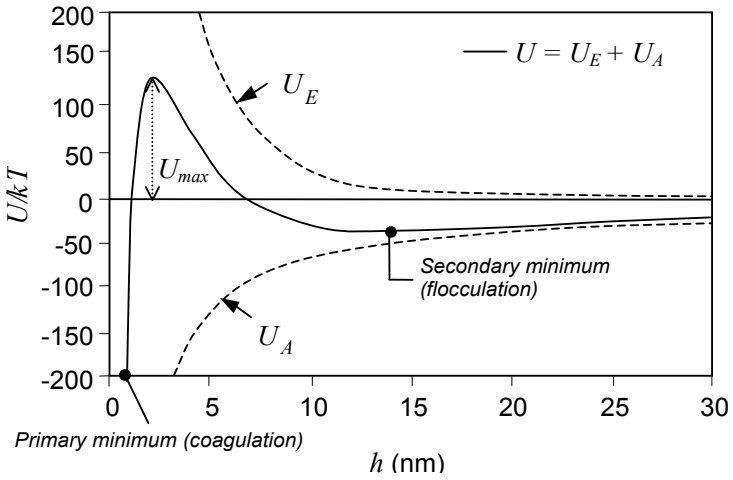

Figure 2-26 Energy of interaction between two droplets (Peña, 2004)

When two droplets get close to each other (h = 0), the attractive forces dictate and droplets are predicted to commingle permanently which is called coagulation. If h reaches secondary minimum energy, then droplets may produce volatile aggregates that can easily re-dispersed, which is called flocculation. This kind of aggregation is considered reversible. Therefore, aggregation is a process that defines either coagulation or flocculation. In case $U_{max} \leq 0$, a fast aggregation happens because there is no energy barrier blocking the two surfaces from getting closer. While if $U_{max} > 0$, there is an energy barrier in between the two surfaces causing a slow aggregation.

2.4.5.3 Coalescence

It describes the mixing of two or more droplets to produce a large droplet. This phenomenon happens when the thin layer of continuous phase between the two droplets vanishes and they cohere instantly to form individual droplet. Thus, the rate of coalescence as well as the properties of the thin layer of the continuous phase affect the stability of an emulsion. Several authors did some experiments and studies to justify the formation and thinning of the flat layer between droplets. One of the explanations is

Weber number that link the internal Laplace pressure P_L and external stress τ_{ext} acting on the two drops:

$$W_e = \frac{\tau_{ext}}{P_L} \quad \textbf{(2 - 12)}$$

If W_e <<1, the stability criterion is predicted as (Walstra, 1990):

$$\frac{d^2U(h)}{dh^2} - \frac{dU(h)}{hdh} > -C\frac{\sigma}{R^2} \quad \textbf{(2 - 13)}$$

The U(h) represents the interaction and repulsion energy in DLVO theory, developed independently by Derjaguin and Landau (1941) in Russia and Verwey and Overbeek (1948) in Neatherland, σ is the interfacial tension and C is a constant greater than 0. In case W_e >>1, a larger layer will compose. The deformation is indulged by bigger droplet sizes and minor interfacial tensions. Therefore, the coalescence is headed by the drainage of the amount of liquid in the layer (Tadros and Vincent, 1983). The layer is called Common black film if the electrostatic repulsion forces are relatively robust to equilibrate the van der Waals attraction and capillary pressure. However, it is called Newton black film if the electrostatic repulsion is frail and low range repulsive forces lead instead (Vrij, 1966).

2.4.6 Demulsification

It is common in crude oil productions accompanied with formation water to produce water-in-oil emulsions. Demulsification is one way of treating crude oil emulsions. It adopts two main methods--chemical and physical. The chemical process involves the addition of an appropriate demulsifier to the existing emulsions whereas the physical method consists of electrical, heating, or mechanical processes such as

centrifugation. The most common used methods in the industry are the thermal chemical technique containing the heating along with the addition of demulsifier and the electrical methods (Lissant, 1993).

2.4.6.1 Chemical Techniques

The objective of using the chemical demulsifier is to deactivate the effect of emulsifying agents which stabilize the emulsions. They weaken the stiff layer at the oil/water interface and merge the water droplets. In order to break an emulsion, an adequate selection of the demulsifier chemical formula, a proper quantity and mixing of chemicals, in addition to an acceptable retention time in treating emulsion are needed to settle water droplets along with the physical technique to expedite and discard the emulsions.

2.4.6.2 Action of Demulsifiers

There are several mechanisms to operate a given demulsifier along with their efficiency (Clariant Oil Services, 2007).

Adsorption: An active demulsifier is used for adsorbing the empty positions as the interfacial layer is extended to terminate the stability of the emulsion. Two significant elements of demusifiers for better absorption procedure are mobility and strong segregating behavior to the interface. Coalescence is a consequence of weakening the treated layer causing the formation of bigger droplets.

Displacement: Besides adsorbing, the demulsifiers also displace the previous stabilizing emulsifiers from the interface eliminating this steric barrier. This mechanism is proved to operate upon sufficient interfacial tension and rheology studies.

Solubility: Current demulsifiers are less soluble in crude oil and firstly coat the interface of slight portions of the water droplets.

Wettability: Demulsifiers wetting some solids at the interface such as asphalts, fine silts, iron oxides or sulfides will cause them to transfer to the oil or water phases. It is more favorable to migrate the inorganic contaminants to the water phase and it can be fulfilled when using an adequate wetting agent. However, if the contaminants are asphalt or wax, it is more preferable to move it to the oil phase to protect the water quality.

2.4.6.3 Selection of Demulsifier

It is very essential to select the correct demulsifer used in emulsion breaking procedure. Demulsifiers are chemical materials that consist of solvents (e,g., benzene, toluene, xylene, short-chain alcohols, and heavy aromatic naphtha), surfactants, flocculants, and wetting agents. The performance of the demulsifiers involves fractional or complete displacement of the original stabilizing materials (polar) of the interfacial layer encircling the emulsion droplets. The displacement affects the properties of the layer such as the interfacial viscosity or elasticity of the protecting layer, hence boosting the destabilization. Sometimes, the chemicals behave as wetting agents and change the wettability of the stabilizing particles causing the emulsion layer to break. There are testing methods to promote the proper demulsifiers such as bottle tests, dynamic simulations, and actual plant tests. These tests provide the appropriate quantity of chemicals to be used. Too little or too high dosage of demulsifier will unresolve the emulsion issue. Excess amount of demulsifier can cause the emulsion to stabilize

instead of destabilizing because it is very active material similar to emulsifier agents. This means it acts like a natural emulsifier at the interface (Kokal, 2005).

2.4.6.4 Chemistry of Demulsifier

Each demulsifier is designed for a specific emulsion type and is not suitable for different types. The chemical formula of demulsifiers consist of polymeric chains of ethylene oxide and polypropylene oxides of alcohol, ethoxylated phenols, ethoxylated alcohols and amines, ethoxylated resins, ethoxylated non-phenols, polyhydric alcohols and sulphuric acid salts (Kokal, 2005). **Figure 2-27** shows a typical chemistry of demulsifiers. The composition of each demulsifier might include a single active component or a combination of the highlighted intermediates in the figure. Hence, there are different kinds in intermediates.

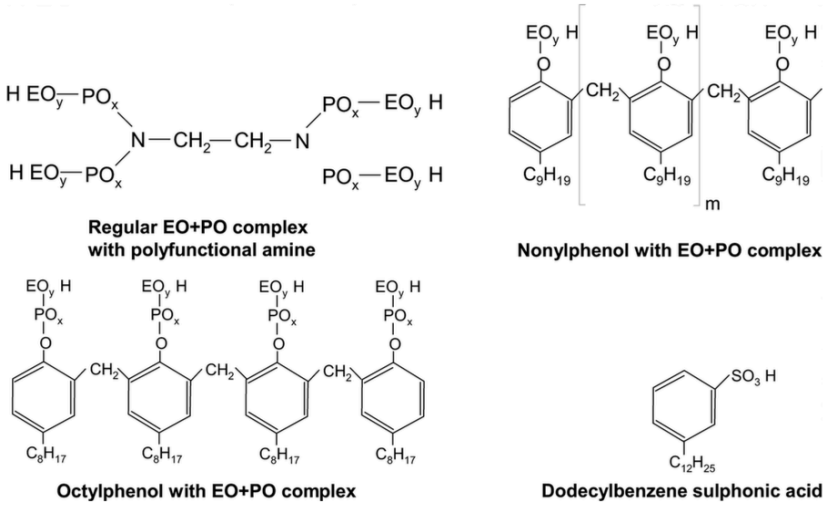

Figure 2-27 Typical demulsifier molecular formulas (EO-Ethylene oxide, PO-Propylene oxide) (Kokal, 2005)

2.4.6.5 Physical Techniques

The physical demulsification methods comprise of heating, electrical, or a mechanical method like centrifugation.

2.4.6.6 Thermal Techniques

In most of the cases, using the heat alone to treat the emulsion does not work unless it is a rare case. Heating treatment is an additional method to improve the separation of emulsion. According to Stokes law, it increases the water settling rate and decreases the viscosity of oil. Also, the thermal energy within droplets increases causing the coalescence frequency between water droplets to increase. On the other hand, there are negative consequences of increasing the temperature such as high cost, loss in light crude oil components which result in reduction in API gravity and potential of scale deposition and corrosion in treating vessels. The selection of heat application is depending on the total economic analysis for the treatment facility. Examples of the heaters used in oil industry include Tubular heaters, fluid-jacket heaters, internal firebox heaters, and jug type heaters (Petroleum Extension Service, 1990).

2.4.6.7 Mechanical Techniques

Mechanical methods using variety of equipment to break oilfield formed emulsion are available such as free-water knock out drums, wash tanks, two-three phase separators, desalters, and settling tank. This technique is designed for low turbulence environment at different settling time depending on the layout of the oilfield (Kokal, 2007).

Table 2-4: Description and application of mechanical equipment for breaking emulsion (Kokal, 2007)

	Equipment	Application	Comments
1	Free water knock out type separator	For high water cut crude oils where the bulk of the water separates out quickly	Final crude polishing to export can be carried out using other methods
2	Dehydration type	For low water cut crudes where dehydration is about 1-5 % water is required	Usually located downstream of FWKO separators in offshore environment
3	Separators	Considered for dehydration of difficult emulsions or very viscous crudes	Choice is based on economic arguments, and can be operated at high temperatures than 100 ^{o}C
4	Heater treaters	General purpose, particularly used for high water cut crudes.	Careful design of internal requirements to avoid channeling and flooding
5	Wash tanks Concentric wash tanks Settling tanks	Particularly used for heavy water cuts General purpose	More expensive and difficult to operate Not a good choice for high water cut crudes
6	Electrostatic Coalescers	Considered when deep dehydration is required (to about 0.5% water)	More sophisticate and more potential problems are experienced

2.4.6.8 Electrical Techniques

Treating emulsion with high voltage electricity is most of the time effective. The water droplets normally contain charge and when inducing electric field, the droplets travel faster, strike each other and merge (Gray and Moshen, 1999). The electric field influences the rigid interfacial layer by redistributing the polar molecules thus attenuating the interface and boosting coalescence. The electrical unit includes transformer and electrodes that deliver high voltage alternating current. The placement of the electrodes gives an electric field perpendicular to the direction of flow. Adjusting the distance between electrodes in some designs provides a variety of voltage values

needed to treat an emulsion. It is uncommon to use the electrostatic dehydration in treating emulsions. It is often applied in combination with chemical and heat treatment. Habitually, it involves loss in heat addition. This reduction in temperature lessens some of the difficulties associated with scale and corrosion formation. **Table 2-4** describes the emulsion treating facilities and their applications.

2.5 Emulsions in Artificial Lift Systems

2.5.1 Emulsion in Gas Lift System

Emulsions are normally found in wells with water cuts ranging from 30% to 60%. Wells with higher water cut might not experience emulsion difficulties but it can suggest using another lifting method because the gas/liquid injection ratio increases with high water cut wells. Literature suggests that the Gas lift technique stimulates emulsion formation due to the mixing action of turbulence applied at the injection point. Production instabilities are caused by emulsions when the gas/liquid ratio increases, as well as several operational problems at surface facilities. Emulsions can ascent the production pressure and decrease the pressure drop across the operating point of injection (prompting subcritical flow through gas lift valves as can been seen in **Figure 2-28**. The calculation of the production pressure down the well using the multiphase flow correlations is imprecise when the fluid is emulsified due to the following:

- The flow pattern is too difficult to predict because it needs an accurate liquid surface tension and other PVT properties that are tough to obtain in the presence of emulsions.
- Unidentified flow pattern indicates that it is impossible to determine the liquid holdup and the corresponding hydrostatic pressure drop.

- It is impossible to calculate the actual friction pressure drop as well due to unknown flow pattern and the difficulty in estimating the viscosity of emulsion (Hernandez, 2016).

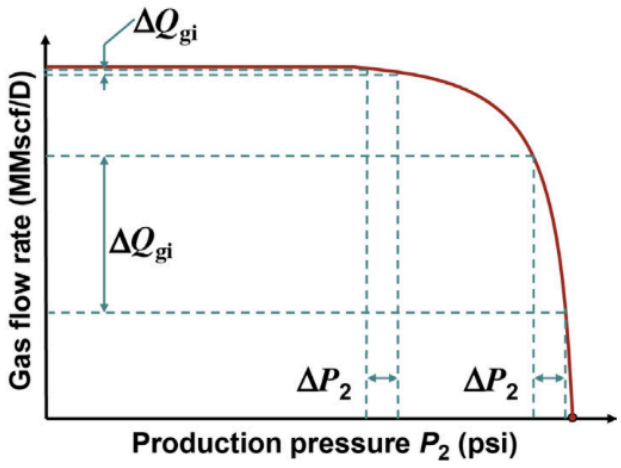

Figure 2-28: Effect of the downstream (production) pressure fluctuation on the gas flow rate across an orifice valve (Hernandez, 2016)

2.5.2 Emulsion in ESP

An extensive literature review on ESP problems was done in 1999 (Lea and Bearden) and the first indication about potential problems reported was as a result of asphaltene deposition. On the other hand, emulsion formation problems are also known when operating an ESP. Zhizhuang and Bassam (2007) reported that in Penglai 19 to 3 offshore oil field (South China Sea) equipped with ESP showed a sharp increase in the viscosity of the produced fluid due to W/O emulsion formation. As a result, a chemical injection line was built-in for emulsion breaker addition. The formation of viscous emulsion was experienced in a number of wells and injecting chemicals downhole was found effective as temporary solution in breaking the formed emulsion. The effect of emulsion formation in ESP has also been considered by Yang et al. (2012). A significant impact of this emulsion phenomenon was found to increase the frictional

pressure drop in ESP wells as a result of the the sharp increase in the viscosity causing many problems to the ESP.

2.6 Two-Phase Vertical Flow Correlations

In oil industry, the emulsion phenomena often occur with water-oil flow. Many investigations have been conducted to study and predict the emulsion phenomenon in such flows. Emulsion is a stable dispersion that involves additional surface active agents (surfactants). The main role of the emulsifying agent is to lower the surface tension which facilitates the break up and inhibits coalescence. However, not many studies have been done concerning the effect of gas injection on emulsion flow. This situation is relevant for the gas lift system. Using this technique, the gas is injected at the bottom of the production tubing (through which fluid is flowing) to decrease the gravitational pressure drop in the well. This helps in increasing the flow rate in the tubing. The process of injecting the gas is operated through a valve attached inside a side pocket mandrel which generates large bubbles. For this case, the emulsion can affect the efficiency of the gas lift system and vice versa. An emulsion is a mixture of oil and water that form a very viscous mixture leading to a high friction with the pipe wall as well as within the fluid and thus increasing the pressure gradient. This is unfavorable while producing oil. In consequence, the flow experiments have been carried out to understand the effect of gas injection on water-oil emulsions in vertical pipes. The following observations are seen regarding the influence of gas injection.

To study the flow characteristics of two phase flow in a vertical loop as the gas is injected through the valve at various rates, the pressure drop was investigated for

constant liquid rate and a range of gas rates. The dispersion that was achieved was a gas in liquid dispersion.

2.6.1 Pressure Gradients

To fully develop the two phase flow, the total pressure gradient in a vertical loop system is equal to the sum of the gravity pressure gradient and the frictional pressure gradient while the kinetic energy pressure drop will be negligible. It is calculated from the difference in velocity over a finite distance of pipe, Δz

$$\frac{dp}{dz} = \left(\frac{dp}{dz}\right)_{gravity} + \left(\frac{dp}{dz}\right)_{friction},$$

(2 - 14)

in which the p is the pressure and z is the vertical coordinate that points in the same direction as gravity. The modified Hagedorn and Brown correlation method is selected for the two phase vertical flow in vertical pipe for liquid holdup calculation; the modification of the original method includes using the no-slip holdup and the use of the Griffith correlation for the bubble flow regime. The potential energy pressure gradient is based on the average density, $\bar{\rho}$,

$$\left(\frac{dp}{dz}\right)_{gravity} = \frac{g}{g_c}\bar{\rho}sin\theta$$

(2 - 15)

where

$$\bar{\rho} = (1 - y_l)\rho_g + y_l\rho_l$$

(2 - 16)

the holdup of the liquid phase is defined identically to y_l as

$$y_l = \frac{V_l}{V}$$

(2 - 17)

where V_l = volume of liquid phase in pipe segment and V= volume of pipe segment. The holdup of the gas phase, y_g, is sometimes called the void fraction

$$y_g = 1 - y_l \tag{2 - 18}$$

in order to find the mixture velocity, the superficial velocity is calculated,

$$u_{sl} = \frac{q_l}{A} \tag{2 - 19}$$

and

$$u_{sg} = \frac{q_g}{A} \tag{2 - 20}$$

then, the mixture velocity that is used in the H-g correlation to calculate the pressure gradient is the sum of the superficial velocities,

$$u_m = u_{sl} + u_{sg} \tag{2 - 21}$$

The correlations are chosen depending on the flow regime from the following. Bubble flow occurs if $\lambda_g < L_B$, where

$$L_B = 1.071 - 0.2218 \left(\frac{u_m^2}{D}\right) \tag{2 - 22}$$

and $L_B \geq 0.13$. Therefore, if the computed value of L_B is less than 0.13, L_B is set to 0.13. If the flow regime happens to be bubble flow, the Griffith correlation is used; otherwise, the original Hagedom-Brown correlation is used.

Flow regimes other than bubble flow: The original Hagedorn-Brown correlation. The form of the mechanical energy balance equation used in the Hagedorn-Brown correlation expressed in oilfield units is

$$144\frac{dp}{dz} = \bar{\rho} + \frac{f\dot{m}^2}{(7.413 * 10^{10}D^5)\bar{\rho}}$$

(2 - 23)

where f is the friction factor, $\dot{m}$ is the total mass flow rate (lb_m/d), $\bar{\rho}$ is the in-situ average density (lb_m/ft^3), D is the diameter (ft), u_m is the mixture velocity (ft/sec), and the pressure gradient is in psi/ft. The friction factor is based on a mixture Reynolds number. The liquid holdup is obtained from a series of charts using the following dimensionless numbers in oilfield units.

Liquid velocity number, N_{vl}:

$$N_{vl} = 1.938\, u_{sl}\sqrt[4]{\frac{\rho_l}{\sigma}}$$

(2 - 24)

Gas velocity number, N_{vg}:

$$N_{vg} = 1.938\, u_{sg}\sqrt[4]{\frac{\rho_l}{\sigma}}$$

(2 - 25)

Pipe diameter number, N_D:

$$N_D = 120.872\, D\sqrt{\frac{\rho_l}{\sigma}}$$

(2 - 26)

Liquid viscosity number, N_L:

$$N_L = 0.15726\,\mu_l \sqrt[4]{\frac{1}{\rho_l \sigma^3}}$$

(2 - 27)

Where superficial velocities are in ft/sec, density is in (lb_m/ft^3), surface tension is in $dynes/cm$, viscosity is in cp, and diameter is in ft. The holdup is obtained from Figure 4-1 through Figure 4-3. First, CN_l is read from Figure 4-1. Then the group

$$\frac{N_{vl} p^{0.1} (CN_L)}{N_{vg}^{0.575} p_a^{0.1} N_D}$$

(2 - 28)

is calculated; from Figure 4-2, we get y_l/ψ. Here p is the absolute pressure at the location where pressure gradient is wanted, and p_a is atmospheric pressure. Then, computing

$$\frac{N_{vg} N_l^{0.380}}{N_D^{2.14}}$$

(2 - 29)

and reading ψ from Figure 4-3. The liquid holdup is then

$$y_l = \left(\frac{y_l}{\psi}\right)\psi$$

The mixture density is then calculated using equation (2 - 16).

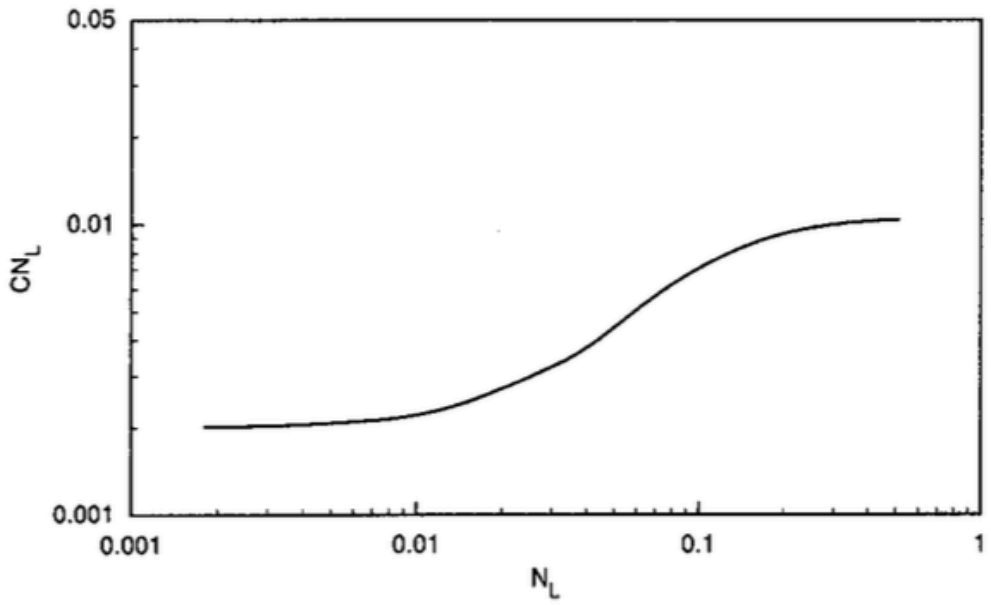

Figure 2-29 Hagedorn and Brown correlation for CNL (from Hagedorn and Brown, 1965)

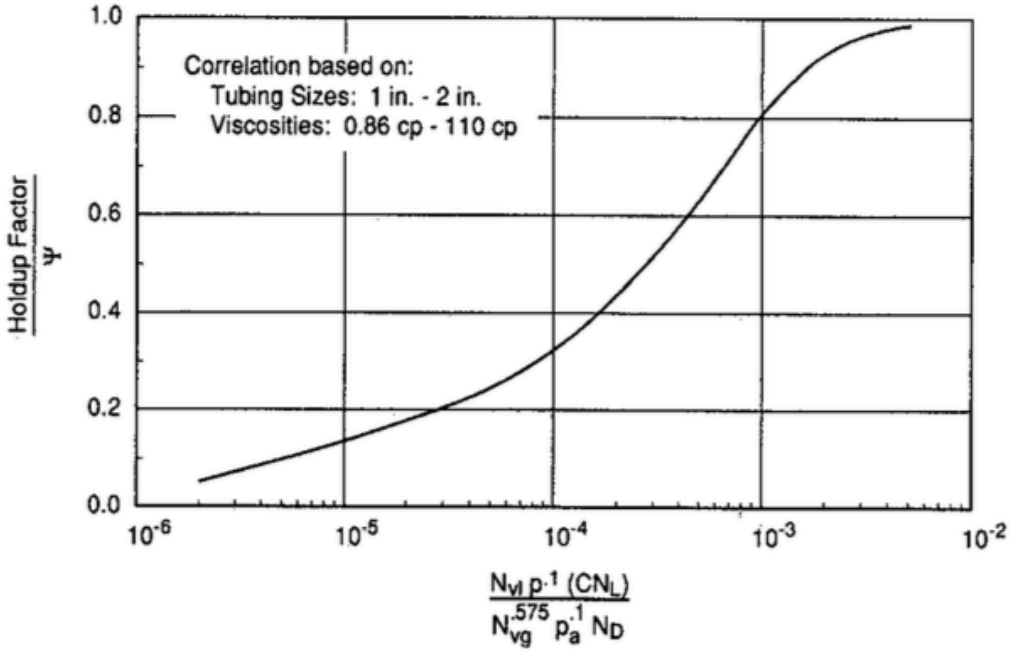

Figure 2-30 Hagedorn and Brown correlation for holdup/ ψ. (from Hagedorn and Brown, 1965)

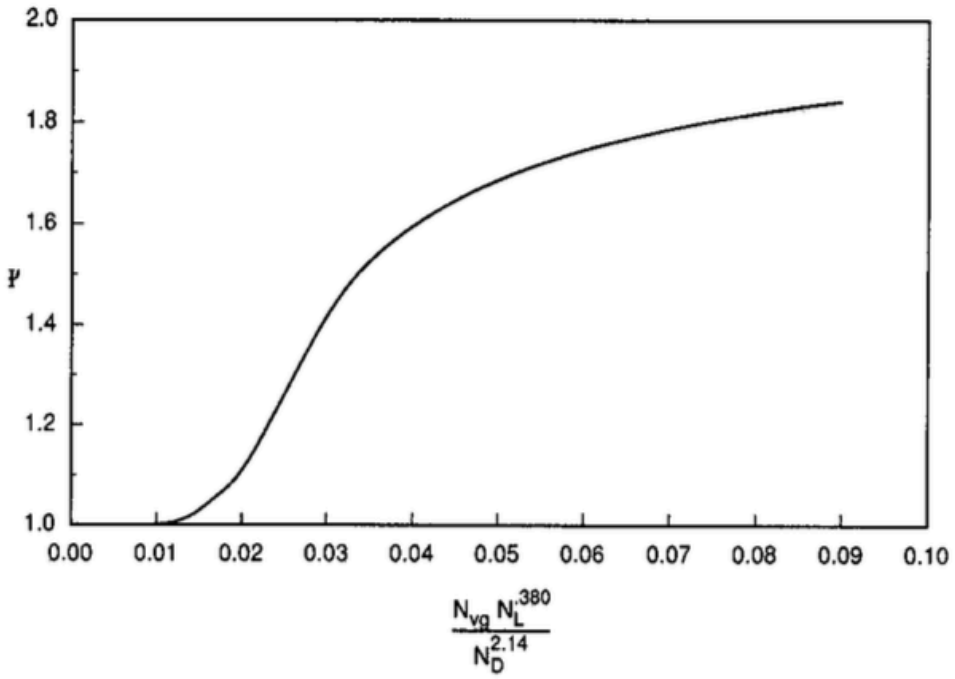

Figure 2-31 Hagedorn and Brown correlation for ψ. (from Hagedorn and Brown, 1965)

The frictional pressure gradient depends on a fanning friction factor using a mixture Reynolds number, written in field units as

$$N_{Re} = \frac{2.2 * 10^{-2}\dot{m}}{D\mu_l^{yl}\mu_g^{1-y_l}} \tag{2 - 30}$$

where mass flow rate, $\dot{m}$, is in (lb_m/day), D is in ft, and viscosities are in cp. The friction factor is calculated with the Chen equation

$$\frac{1}{\sqrt{f_f}} = -4log\left\{\frac{\epsilon}{3.7065} - \frac{5.0452}{N_{Re}} log\left[\frac{\epsilon^{1.1098}}{2.8257} + \left(\frac{7.149}{N_{Re}}\right)^{0.8981}\right]\right\} \tag{2 - 31}$$

for the calculated Reynolds number and the pipe relative roughness

$$\epsilon = \frac{k}{D}$$

(2 - 32)

where k is the length of the protrusions on the pipe wall and D is the pipe diameter.

Bubble flow: The Griffith correlation. The Griffith correlation uses a different holdup correlation, bases the frictional pressure gradient on the in-situ average liquid velocity. For this correlation the pressure gradient in oilfield units,

$$144\frac{dp}{dz} = \bar{\rho} + \frac{f\dot{m}_l^2}{(7.413 * 10^{10}D^5)\rho_l y_l^2}$$

(2 - 33)

where m_l is the mass flow rate of the liquid only. The liquid holdup is

$$y_l = 1 - \frac{1}{2}\left[1 + \frac{u_m}{u_s} - \sqrt{\left(1 + \frac{u_m}{u_s}\right)^2 - 4\frac{u_{sg}}{u_s}}\right]$$

(2 - 34)

where $u_s = 0.8\ ft/s$. The Reynolds number used to get the friction factor is depending on the liquid mass flow rate and viscosity (Economides, 2012).

$$N_{Re} = \frac{2.2 * 10^{-2}\dot{m}_l}{D\mu_l}$$

(2 - 35)

Chapter 3. Experimental Design

Very few studies have been conducted on gas lift in vertical flow pipe in the presence of emulsions. Most of the published work focuses on the study of emulsion behavior in vertical or inclined pipe. This chapter summarizes the development of the desired experimental design and the final modifications as well as the sets of experiments conducted using a vertical flow loop system with a simulated gas lift unit. The first set examines the pressure drop required to lift water while increasing gas rates in the two phase water-gas system. Then, a comprehensive comparison with the second series of experiments conducted with the oil-gas system is presented. Later, we share the modifications made on the system for conducting emulsion tests due to some limitations with the original setup.

3.1 Description of Experimental Setup

The design of the laboratory apparatus comprises of three components, the first part models the well-reservoir coupling, the second is the gas injection system, and the third is the production tubing of the three phase system. The three phase loop system is approximately 10 ft high. The initial setup was built with an internal pipe diameter of ¼ in made of plastic tested with turbulent flow regime. Gas was injected at the bottom using a gas valve. At this stage, liquid was injected at constant pressure using a positive displacement pump. Due to the limitation in witnessing variations in the flow regimes, the pipe was upgraded to ¾ in plastic pipe and the pump was replaced by a centrifugal pump (forced convection) to achieve higher flow rates. The loop was continuously filled with liquid at the desired rate before taking measurements. For more accurate

pressure measurements, a pressure transducer was connected at the bottom of the pipe. The gas injection was not effective in this system which resulted in further modifications as shown in **Figure 3-1**.

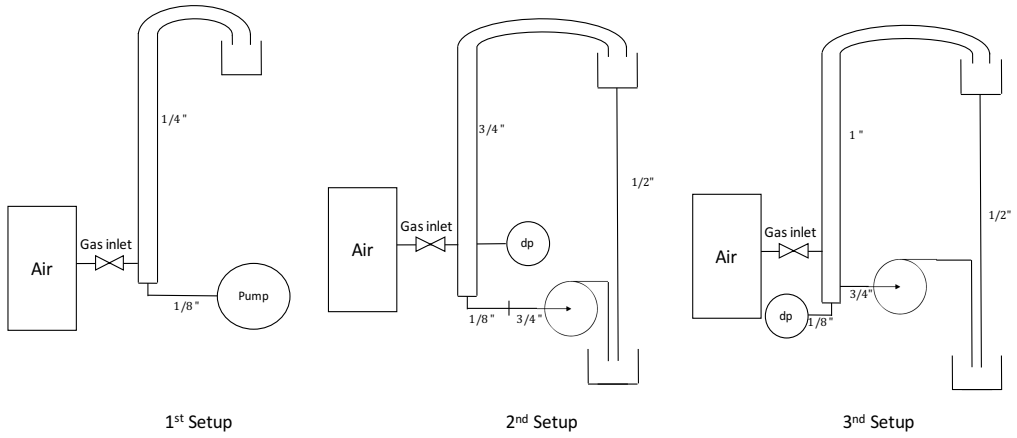

Figure 3-1 Sketch for the early stages in the optimization of the flow loop design

3.1.1 Experiments Setup and Procedure for Water/Gas and Oil/Gas Flow

The final design of the flow loop apparatus is a 1 in internal diameter pipe, the top 8 ft are made out of durable clear polycarbonate and the bottom 2 ft are stainless steel. Air is injected at the bottom at h= 2 ft through a gas injector-nozzle centered in the middle of the vertical pipe creating different sizes of bubbles, small and large, depending on the injection pressure (**Figure 3-2**). A pressure transducer is located at the bottom of the testing tube at h = 1 ft. The pressure measurements were precise with a relative uncertainty range of 0.5%. The liquid flow rate is created by a centrifugal pump (forced convection). The loop is continuously filled with liquid at the desired rate before taking measurements. The volumetric flow rate is measured manually at the top part of the loop where it is open to the atmosphere. The experiments are conducted at room temperature values between 20^{o}C and 25^{o}C, such that the viscosity change is insignificant and the results are reproducible.

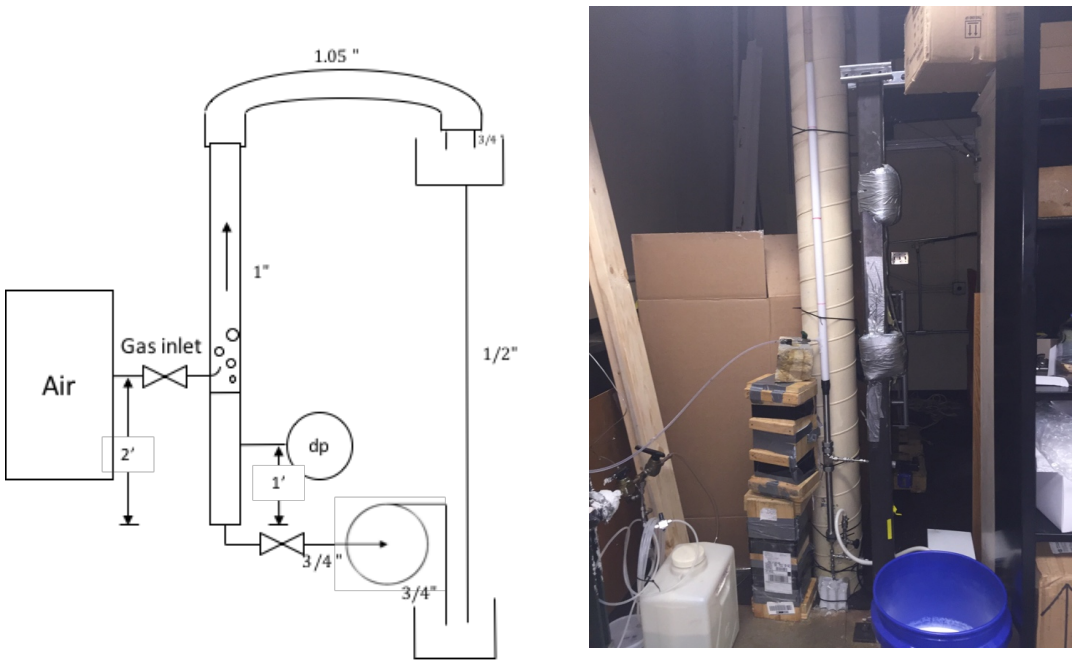

Figure 3-2 Sketch and picture of the water and oil final vertical flow loop setup

3.1.1.1 Procedure:

The experiment is run using three pump speeds (low, medium, high) with each speed the water is pushed inside the tubing, gas is injected at various rates and collected at the top for accurate rate measurements. The pressure is recorded for each gas flow rate. Respectively, the experiment is repeated using oil following the same procedure outlined above for water. All the experiments were performed at room temperatures between 20^{o}C and 25^{o}C, so the change in viscosity is insignificant.

3.1.2 Setup for Emulsion Flow

The setup for emulsion was modified due to few encountered problems, see **Figure 3-3**. The centrifugal pump increased the viscosity of emulsion making it difficult to pump in addition to maintaining enough head for the pump to operate. The modified setup includes three active components. The first part is made of a 2 liters accumulator filled with emulsion modeling the well-reservoir coupling, the second is

the gas injection system, and the third is the production tubing of three phase system. The liquid was injected at constant rate using two connected pumping units to give a sufficient liquid flow rate.

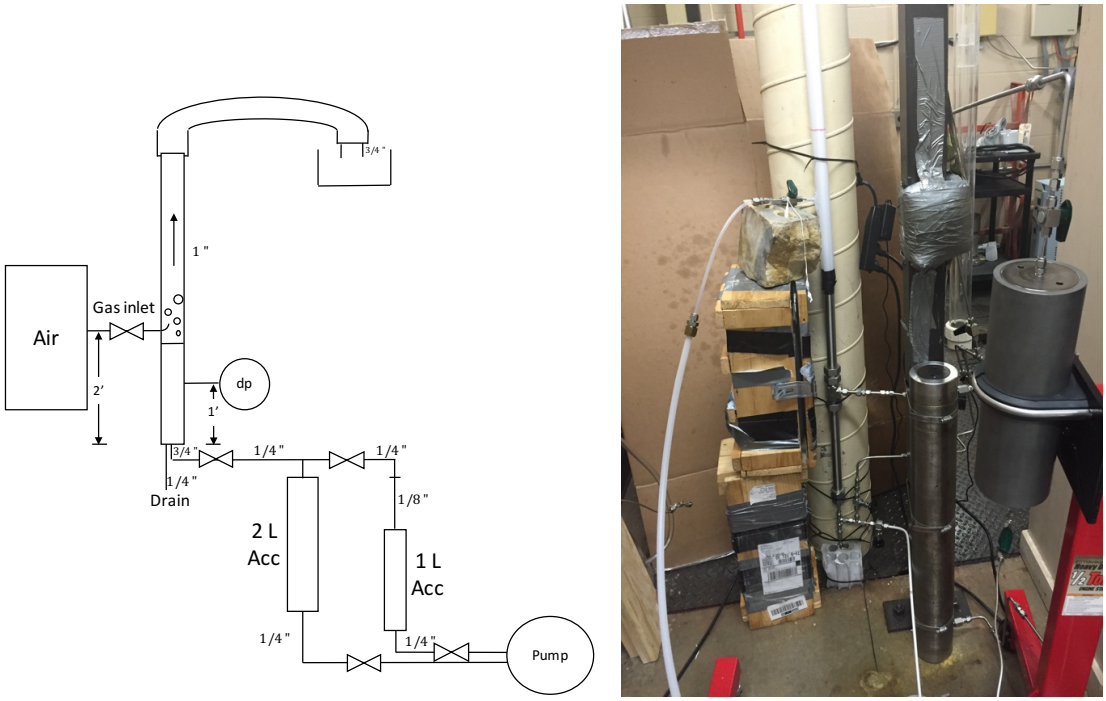

Figure 3-3 Sketch and picture of the emulsion lab setup

3.1.2.1 Emulsion Formation:

To create a stable water-oil emulsion needed for the experiment, several samples were created using different water cut and surfactant percentage. The examined water cuts were 20%, 30%, 40% and 50% while the surfactant percentages were 1%, 1.5% and 2%. 70% oil and 30% water are emulsified using a 2% mixture of span-80 and Merpol surfactants diluted in oil before adding the water then stirred for 30 minutes resulting in a stable water-oil emulsion. The total volume of water-oil emulsion was 11 liters. For the water-oil emulsion pipe flow, the in-line mixture viscosity was measured before and after each gas injection rate. The value changes due to the several factors

such as changes in drop size. Moreover, the viscosity of the emulsion was measured daily since the experiment took a week to be completed.

3.1.2.2 Procedure:

The two liters accumulator was filled using a one liter accumulator (in two rounds) linked to the connected pump units. The constant liquid flow rate was generated from the pumping units to fill the tubing. After the pressure stabilized, the gas was injected at different rates and collected at top for measurements meanwhile the pressure was recorded. Also, the emulsion's viscosity is measured for each injected gas flow rate.

Chapter 4. Experimental Results and Analysis

Studies of emulsion inside a production system that includes artificial lift system are very limited. The gas lift technique is often introduced during oil production to reduce the pressure drop of a vertical liquid column enhancing the production. Whereas the ESP enhances production by adding energy to the fluid lifting it to the top. There is evidence from the field that for certain conditions the gas lift and ESP techniques have influence on boosting the formation of emulsions. The initial two phases of the experiment were to certify that the setup we built for gas lift was working. The third phase was to investigate the influence of gas injection into an water-oil emulsion flow through a vertical production tube as well as the changes in emulsion properties as it goes through the centrifugal pump. Such processed can change viscosity of the emulsion.

4.1 Fluids and Chemicals

The fluids used were dry air, deionized water, and mineral oil. To emulsify the oil and water chemicals such as Span 80 and Merpol surfactants were consumed. A summary of fluid and chemicals data for the experiments is illustrated in **Table 4-1**.

Table 4-1: Fluid and chemical data

Fluid Properties	
Water	Tap water = 1000 kg/m^3 = 1 cP $\gamma_{water/air}$ = 72.8 mN/m
Oil	= 794 kg/m^3 = 30.46 cP $\gamma_{oil/air}$ = 30.1 mN/m
Air	= 1.2041 kg/m^3 = 1.983*10^{-2} cP
Span-80	Nonionic surfactant = 994 kg/m^3 = 1000-2000 cP HLB = 4.3
Merpol	Nonionic surfactant = 960 kg/m^3 = 24 cP HLB = 13.0
Emulsion	W/O = 909 kg/m^3 = 109.79 cP HLB-blend = 8.65 $\gamma_{emulsion/air}$ = 28.2 mN/m

4.2 Results for Diameter Optimization

The results for the initial experimental setup with ¼ in internal diameter tubing are shown in **Table 4-2** below for water injection. The rate was monitored on the pump and the height of the fluid as it was rising in the tubing was measured.

Table 4-2 Experimental data for the initial lab setup

P (psi)	q (ml/min)	h (ft)
19	3.50	4.75
	2.50	5
	1.90	5.75
	1.50	6.25
	0.815	6.5
	0.533	6.75
	0.156	7
	0	7.25

After running the un-calibrated pump at a constant pressure of 19 psi, the liquid was injected from the accumulator to the production tubing reaching several heights until it stabilized at height of 7.25 ft. The gas injection inside the small vertical loop was simply slug flow at both low and high gas flow rates in addition to inaccurate pressure measurements of the system due to the use of mineral oil in the pump to displace water. Consequently, the system was optimized to the second setup with internal diameter to ¾ in and replacing the positive displacement pump with a centrifugal pump. The results for the system are displayed in the following figures. In **Figure 4-1**, the gas volume fraction is plotted against the calculated Hagedom-Brown pressure correlation and measured pressure. Comparing the measured pressure and calculated for the high speed pump, the percentage of error is high due to the placement of the pressure transducer in front of the gas valve; pressure was increasing as the gas rate increased. The liquid flow rates shown in **Figure 4-2** was very low given the high pump capacity (20 LPM) due to the restriction in one of the connections being 1/8 in between the pump and the production tubing.

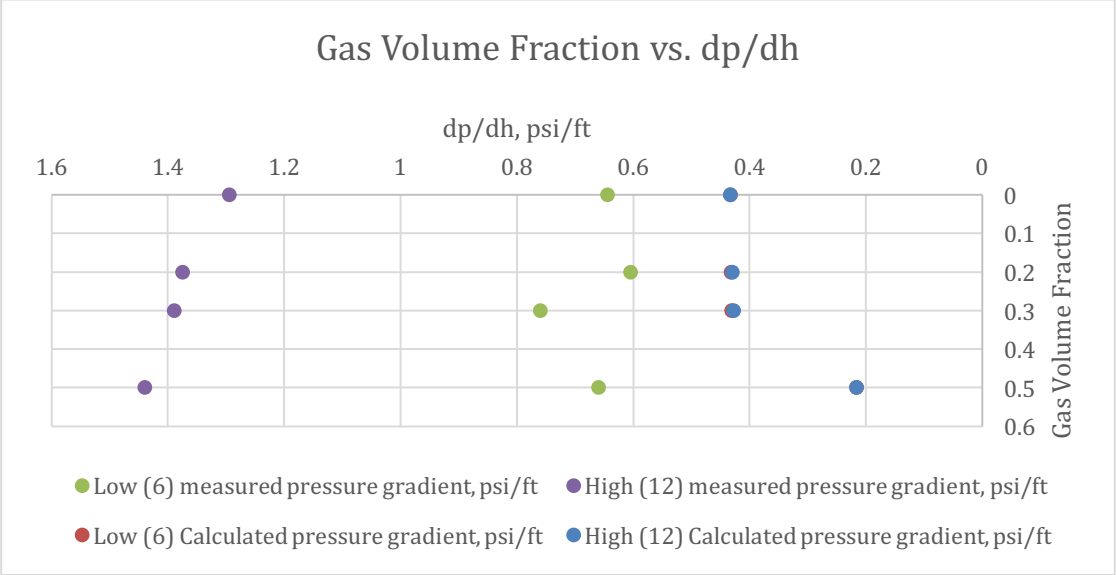

Figure 4-1 Gas volume fraction versus pressure gradient for second lab setup

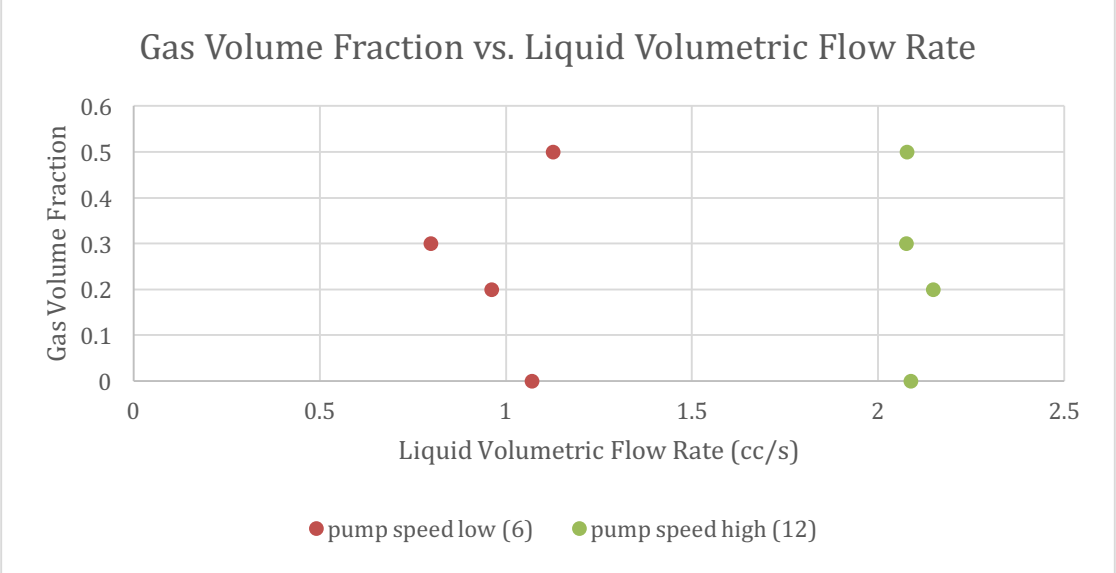

Figure 4-2 Gas volume fraction versus liquid volumetric flow rate for second lab setup

The third experimental setup was modified by upgrading the internal diameter of the tubing to 1 in? and placing the pressure transducer at the bottom of the setup. The following graphs were obtained after running an experiment. From **Figure 4-3** we can see that pressure gradients were slightly improved but still showing a great error

compared to the calculated ones especially for the medium speed pump. And after fixing the restriction in connection and increasing the internal diameter of production tubing, the liquid flow rate achieved was higher. Still, modifications were to be made to fix the pressure gradient as well as increasing the liquid flow rate in order to create a turbulent flow similar to the real field scale.

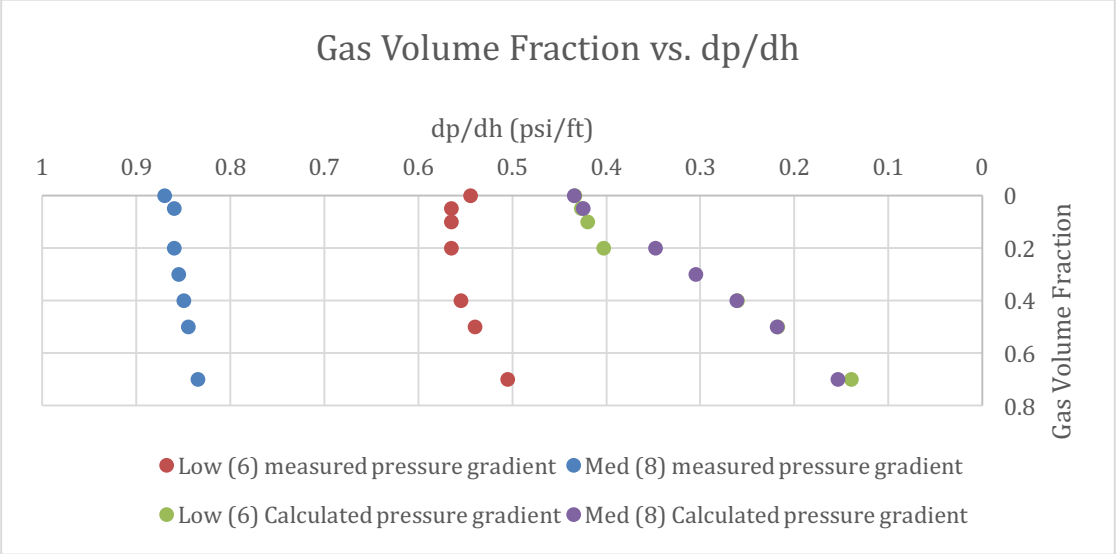

Figure 4-3 Gas volume fraction versus pressure gradient for third lab setup

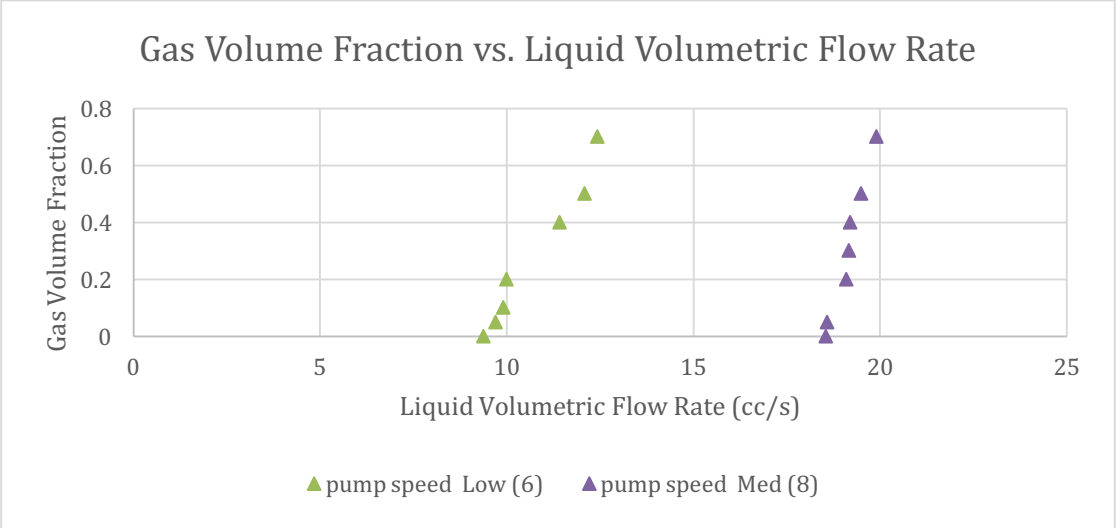

Figure 4-4 Gas volume fraction versus liquid volumetric flow rate for third lab setup

4.3 Results for Water Lift and Oil Lift

4.3.1 Water Lift Results

The results from the final modification on water lift setup are represented in the following figures. In **Figure 4-5**, the liquid flow rates were relatively constant throughout the experiment even after increasing the injected gas rate. Obtaining the decline in the pressure in **Figure 4-6** as the injected gas rate proves the reduction in the density of liquid column for both speeds of the pump. After repeating the same experiment, the obtained results were matching to the previous ones.

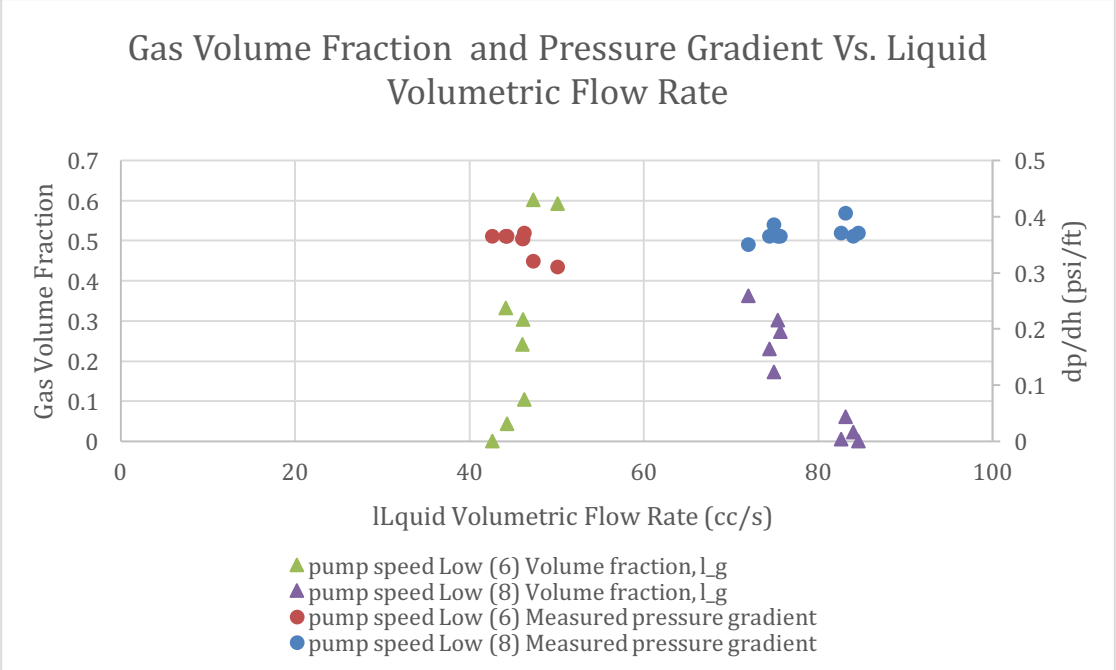

Figure 4-5 Gas volume fraction and pressure gradient versus liquid volumetric flow rate for water lift experiment

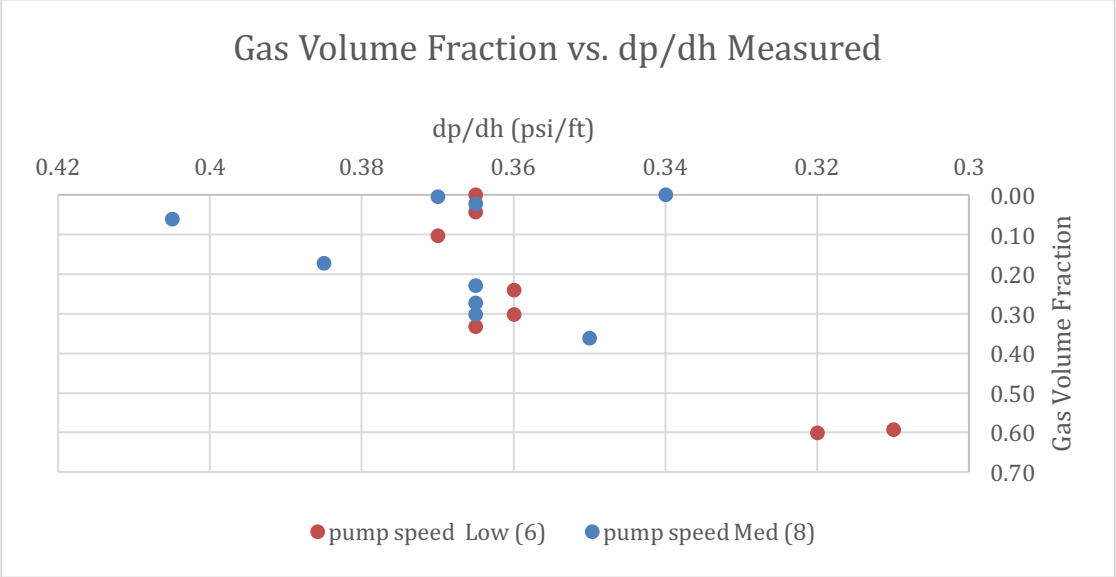

Figure 4-6 Gas volume fraction versus measured pressure gradient for water lift experiment

4.3.2 Oil Lift Results

The last modified setup utilized for water experiment was used to run oil experiments. The viscosity of the mineral oil was 30 cP thus the selected speed of the pump was higher compared to the one in water. The initial test was to examine the optimum speed applicable for the experiment and **Table 4-3** displays that the medium speed (8) was the best. The results achieved from running the oil lift experiment are shown in **Figure 4-7** and **Figure 4-8**. The liquid flow rates were nearly stable around 45 cc/s while the pressure was dropping as more air was injected to the system producing more oil to the surface.

Table 4-3 The liquid flow rates for each pump speed

pump speed	measured pressure gradient (psi/ft)	liquid volumetric flow rate (cc/s)
Low (6)	0.33	16.06
Med (8)	0.365	45.93
High (12)	0.39	65.54

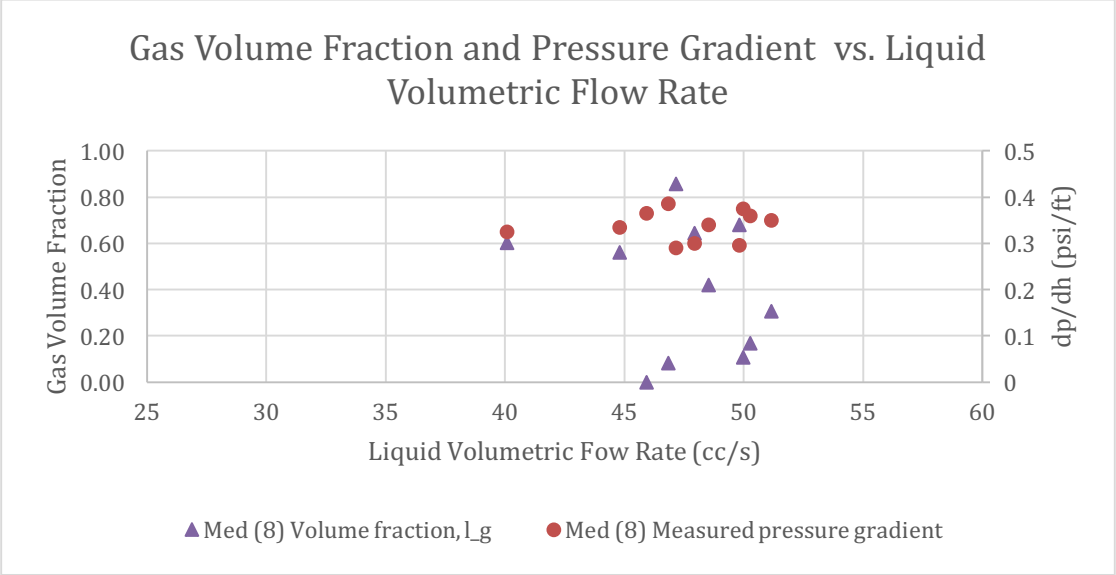

Figure 4-7 Gas volume fraction and pressure gradient versus liquid volumetric flow rate for oil lift experiment

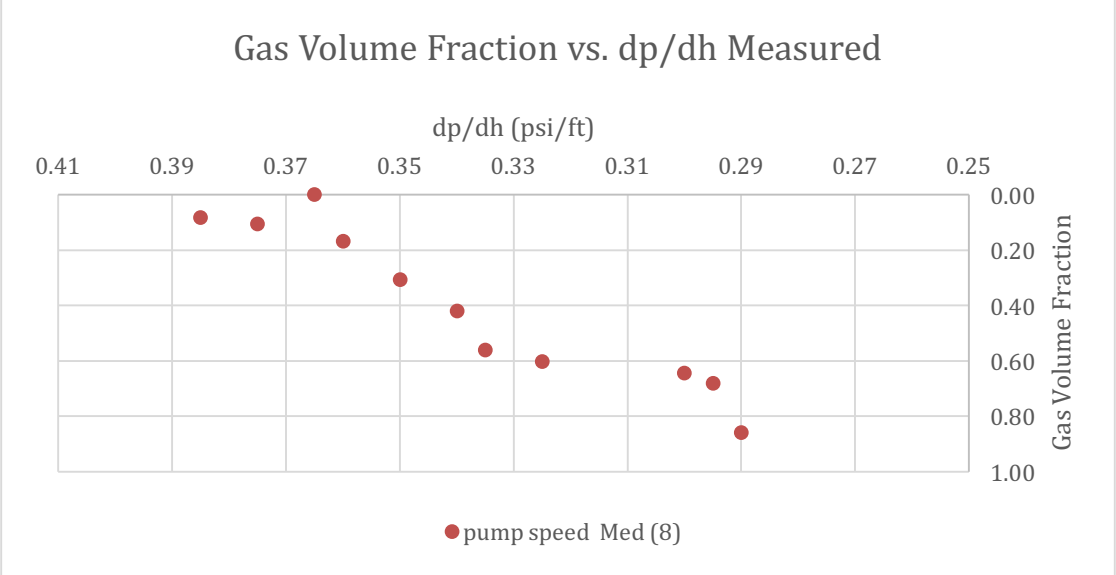

Figure 4-8 Gas volume fraction versus pressure gradient for oil lift experiment

4.3.3 Analysis and Comparison to Correlation

After running several experiments for both water and oil, the data attained are satisfying the purpose of gas lift system. The decline pattern in pressure curves as the gas volume fraction increases are achieved due to the density reduction of the fluid in

the vertical tube. The pressure records were then compared to the pressure calculated from correlation for two phase flow system in vertical pipes.

4.3.3.1 Water to correlation

The pressures are within the range of the calculated ones but the correlation for higher gas rates gives lower pressure gradient and lower gas rates gives higher pressure gradient compared to the measured ones, see **Figure 4-9** for reference. The liquid rates in **Figure 4-10** are consistent while varying the gas rates.

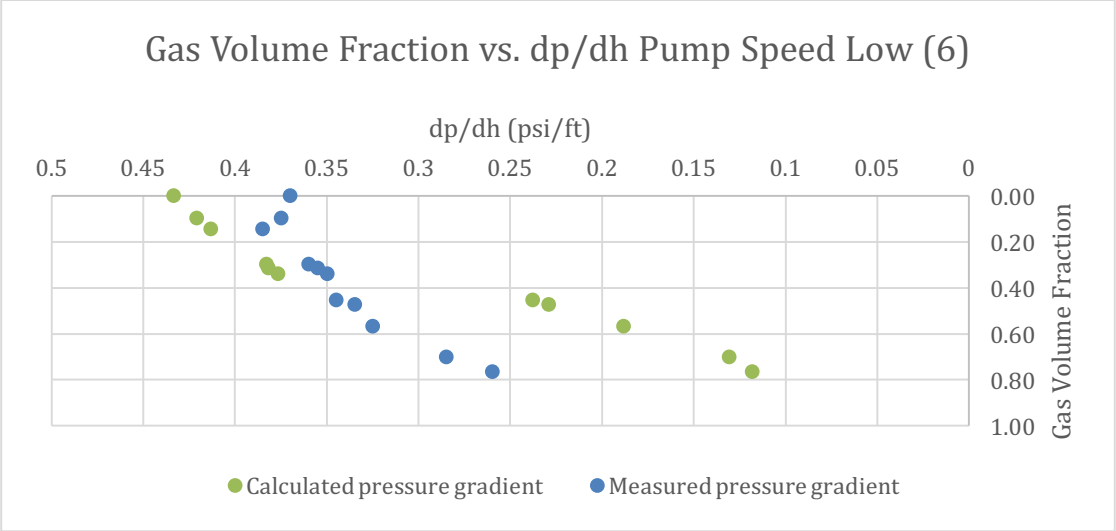

Figure 4-9 Comparison between measured and calculated pressure gradients for water

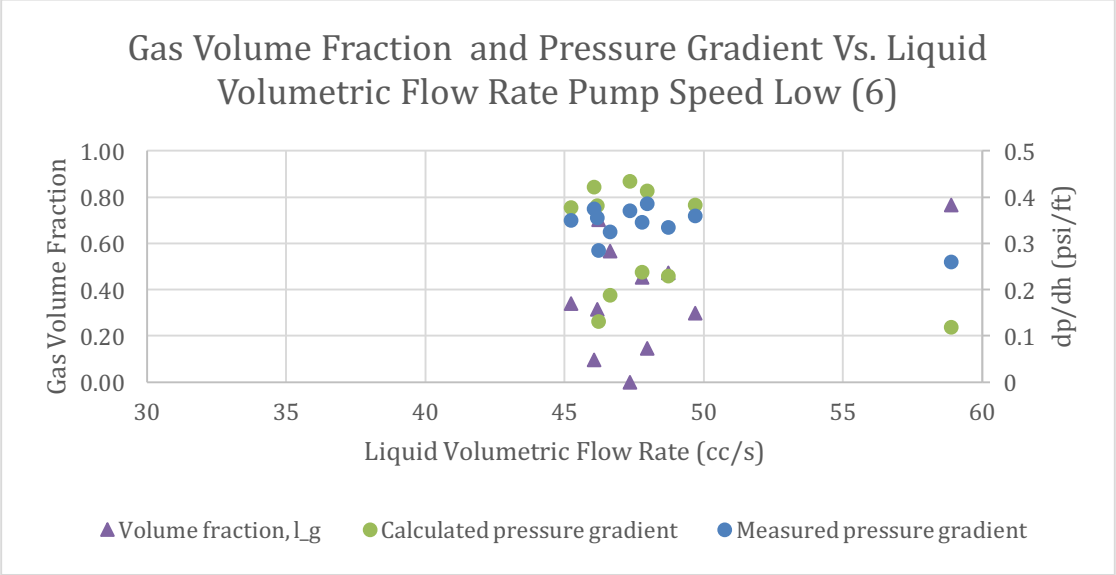

Figure 4-10 Gas volume fraction and pressure gradient (calculated and measured) versus liquid volumetric flow rate

4.3.3.2 Oil to correlation

Similarly, to water, the pressure gradients are within the range of the calculated ones but the correlation for higher gas rates gives lower pressure gradient compared to the measured ones. At zero gas rate, the slight deviation of pressure gradient might be due to the pressure did not stabilize during the measurement, see **Figure 4-11** for reference. From **Figure 4-12**, the liquid flow rates are nearly constant when varying the gas rates.

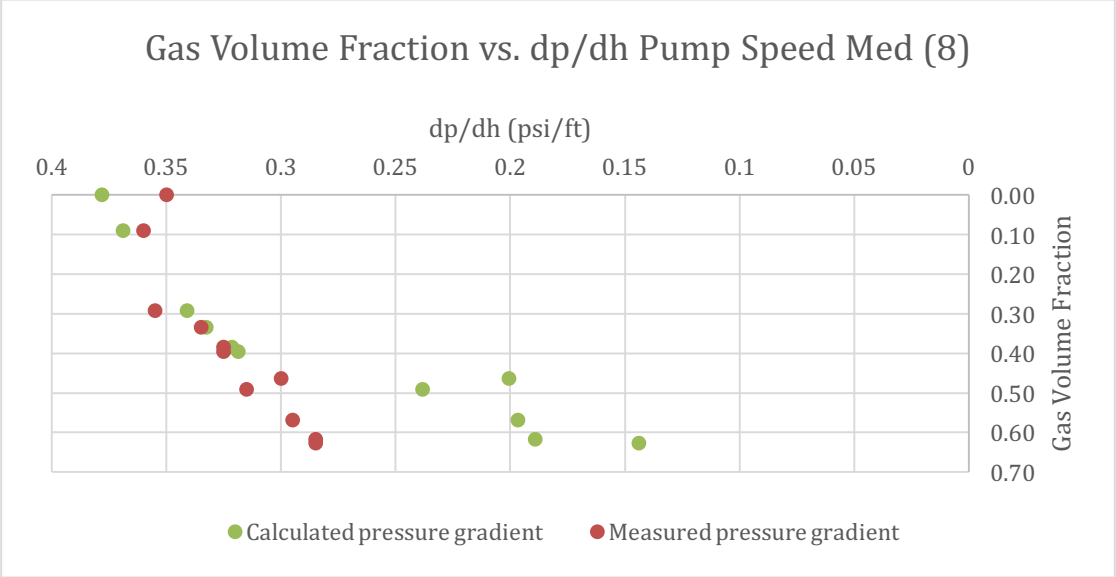

Figure 4-11 Comparison between measured and calculated pressure gradients for oil

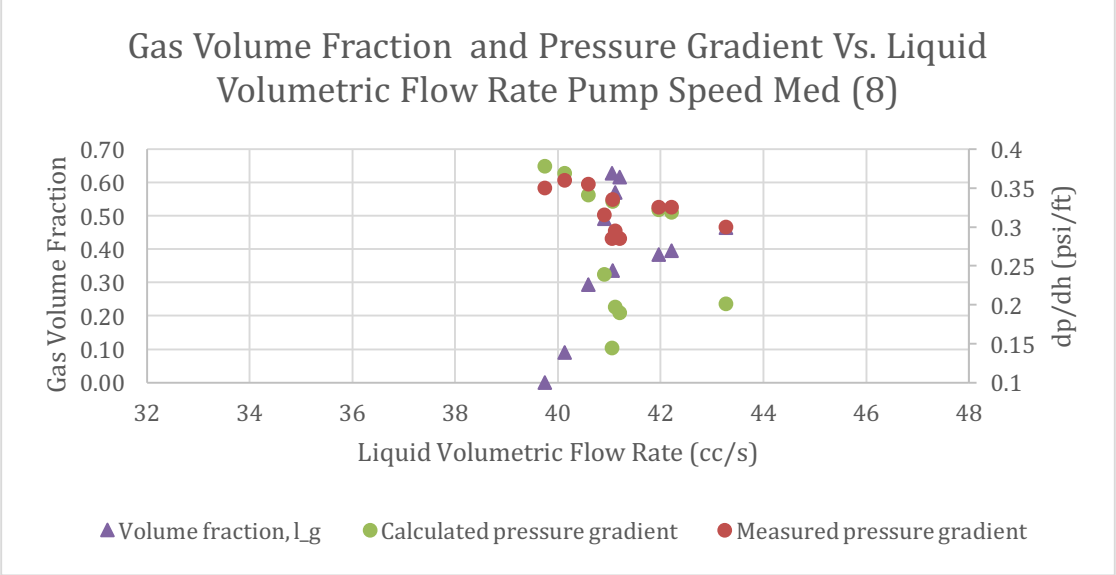

Figure 4-12 Gas volume fraction and pressure gradient (calculated and measured) versus liquid volumetric flow rate for oil

4.3.3.3 Oil to Water comparison

Comparing the results obtained from water and oil, **Figure 4-13** exhibits similar pattern for the oil and water pressure gradients but the oil pressure gradients were

extended for relative high gas volume fraction unlike the water. Keeping in mind that the pressures were nearly equal at equal gas volume fraction.

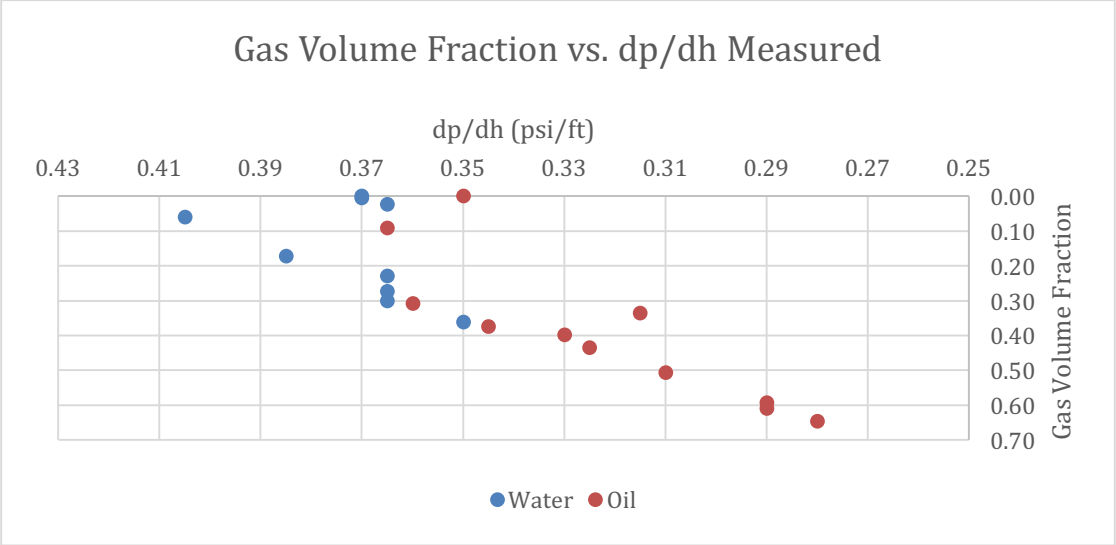

Figure 4-13 Gas volume fraction versus pressure gradient for both water and oil at the same pump speed med (8)

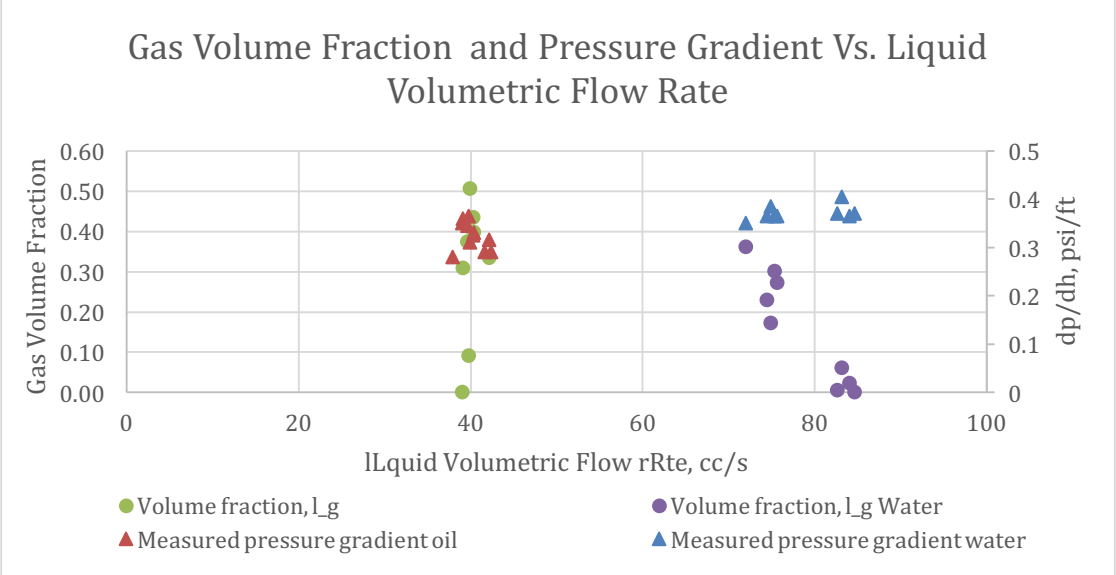

Figure 4-14 Gas volume fraction and pressure gradient versus liquid volumetric flow rate for water and oil lift experiments at same pump speed med (8)

At the same pump speed, the liquid flow rates for water are higher than the oil due to the viscosity difference, see **Figure 4-14**.

4.4 Emulsion Stability and Properties

The factors considered in creating emulsions are water cut %, and chemicals. Several samples were created to test the stability of emulsions with time. The following table summarize the samples data.

Table 4-4 The data for emulsion samples

Sample	%O	%W	%S	Surfactant	Viscosity, cp	HLB	Emulsion Type
1	80%	20%	2%	span 80	54.81	4.3	W/O
2	80%	20%	1%	span 80 + Merpol	57.86	8.65	W/O
3	70%	30%	2%	span 80	200.88	4.3	W/O
4	70%	30%	1%	span 80 + Merpol	77.70	8.65	W/O
5	70%	30%	1.5%	span 80 + Merpol	97.04	8.65	W/O
6	70%	30%	2%	span 80 + Merpol	486.14	8.65	W/O
7	70%	30%	1%	span 80	108.75	4.3	W/O
8	60%	40%	1%	span 80	358.94	4.3	W/O
9	55%	45%	2%	span 80	2036.67	4.3	W/O

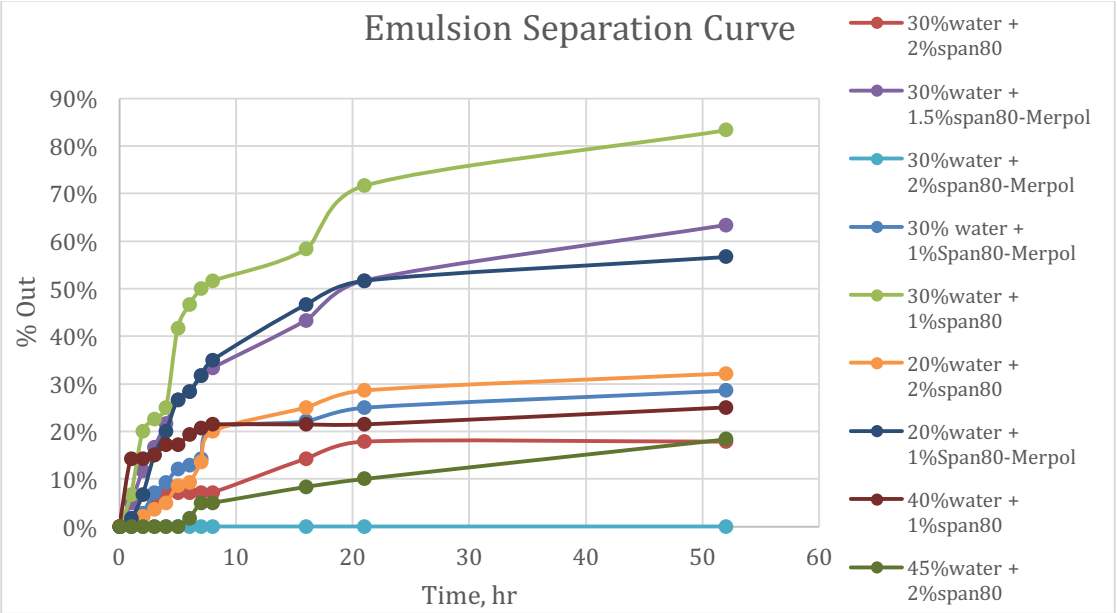

Figure 4-15 The stability test for emulsions

From **Figure 4-15**, the most stable emulsion sample is number 6 with 30% water cut and 2% of mix surfactant. The HLB of the surfactants blend is 8.65 classifying the

emulsion as water-oil emulsion. The dynamic viscosity of the sample was 486.14 cp which is very high compared to the viscosity of mineral oil.

4.5 Results for Emulsion Lift

To run the emulsion lift experiment, the total volume of the created emulsion was 11 liters. The viscosity measurements of the created W/O emulsion are shown in **Table 4-5**, measured for a sample taken every time 4 liters are added to the bucket:

Table 4-5 The viscosity measurements for every few liters of emulsion mixed

Date	Volume, Liters	Time, s	Kinematic Viscosity, cSt	Dynamic Viscosity, cp
8-Jun-16	4	408.62	501.38	455.75
8-Jun-16	8	539.50	661.97	601.73
8-Jun-16	10	353.31	433.51	394.06
8-Jun-16	11	206.59	253.49	230.42

While the density of the dispersion changes linearly with respect to the phase volume fraction, its viscosity undergoes a more complicated behavior causing the difference in viscosities in the table for the same recipe. The main difficulty is that the mixture viscosity depends on the viscosity of the pure phases, the phase fraction, the drop size, the chemical additives, and the general structure (simple or multiple dispersion). The final value of 230 cp is the viscosity for the emulsion that was used in the vertical flow loop.

4.5.1 Effect of Time on Emulsion Viscosity

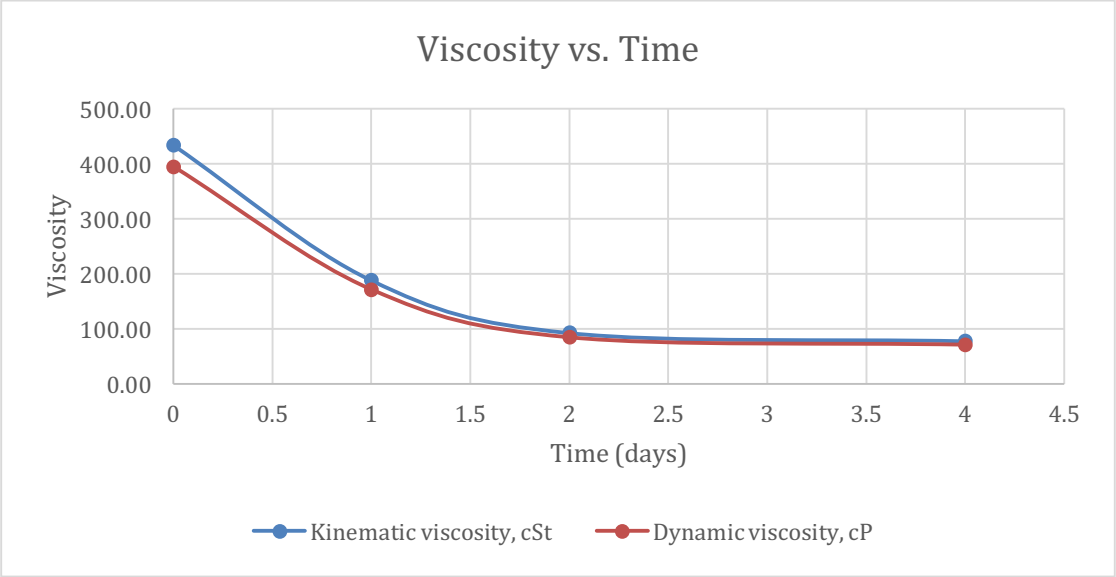

Figure 4-16 Viscosity versus time for W/O emulsion (1)

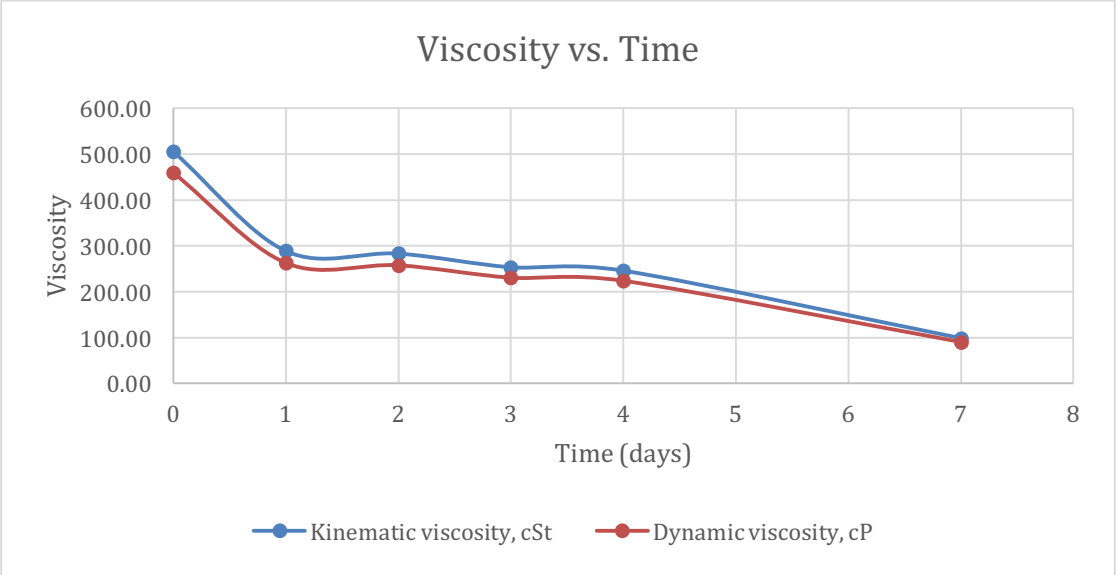

Figure 4-17 Viscosity versus time for W/O emulsion (2)

The viscosity of created W/O emulsion was measured daily. **Figure 4-16** and **Figure 4-17** show the decline in viscosity with time. An emulsion's characteristics change continually from the time of formation to the instant of complete resolution. Accordingly, aged emulsions can exhibit very different characteristics from those that

fresh samples do. This is because any given oil contains many types of adsorpable materials and because the adsorption rate of the emulsifier and its persistence at the interface can vary.

4.5.2 Effect of Centrifugal Pump on Emulsion Viscosity - Results and Implications

After running the emulsion through the pump upon starting the experiment, the W/O emulsion's viscosity increased significantly developing a more stable emulsion, see **Table 4-6**. The obtained results confirm the effect of an ESP on the stability of the formed emulsions during the oil production.

Table 4-6 The viscosity of W/O emulsions before and after running through pump

Date	Original		1st Pump Run		2nd PumpRun	
	Kinematic viscosity, cSt	Dynamic viscosity, cp	Kinematic viscosity, cSt	Dynamic viscosity, cp	Kinematic viscosity, cSt	Dynamic viscosity, cp
8-Jun-16	433.51	394.06	1408.14	1280		
9-Jun-16	187.9	170.8	1227.96	1116.21		
10-Jun-16	92.5	84.08	597.65	543.26	2581	2346.13
12-Jun-16	77.72	70.65	680	618.12	837.64	761.42

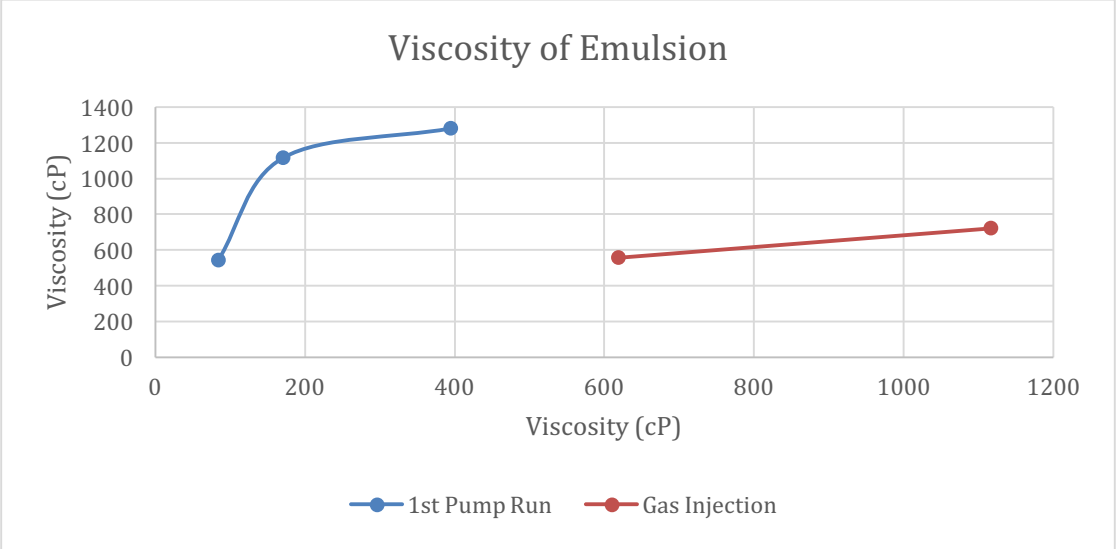

Figure 4-18 The viscosity plot of the pumped emulsion versus the original viscosity of emulsion and the viscosity of emulsion after injecting gas versus the viscosity of pumped emulsion

4.5.3 Effect of Gas Lift on Emulsion Viscosity - Results and Implications

As mentioned the aim of this study is to investigate the influence of gas (air) injected on emulsion flow through a vertical tube. Particular attention is paid to the influence of the injected gas on the viscosity of the emulsion and on the pressure drop over the tube. The viscosity of produced fluid decreased after injecting gas as can be seen in **Figure 4-19**. This may be due to the change in turbulence at higher mixture velocities. More detailed experiments are needed to confirm this assumption.

Table 4-7 The effect of gas injection on emulsion viscosity

Emulsion experiment	**Flow Pattern**	Volume fraction, l_l	Volume fraction, l_g	liquid volumetric flow rate (cc/s)	gas volumetric flow rate, (cc/s)	Dynamic viscosity, cp
	-	1.00	0.00	1.67	0.00	109.76
	bubble	0.08	0.92	1.67	20.34	109.37
	slug	0.02	0.98	1.67	65.62	105.51
	slug	0.02	0.98	1.67	83.64	103.10
	slug	0.01	0.99	1.67	129.48	99.92

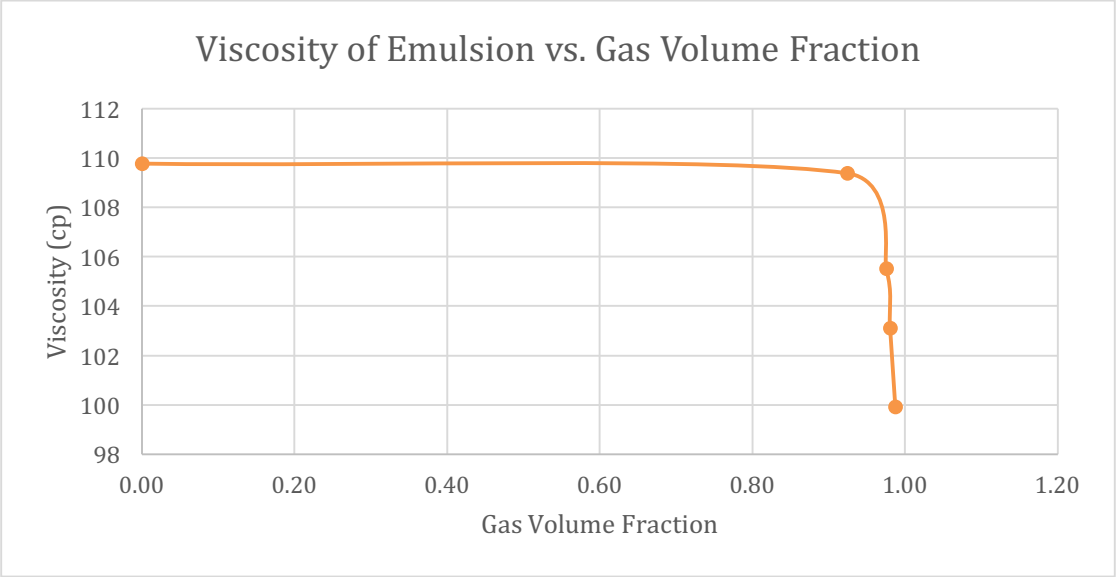

Figure 4-19 Effect of gas injection on the viscosity of emulsion

Table 4-8 The viscosity of W/O emulsions before and after injecting gas

Date	Original		1st Pump Run		Gas Injection	
	Kinematic viscosity, cSt	**Dynamic viscosity, cP**	**Kinematic viscosity, cSt**	**Dynamic viscosity, cP**	**Kinematic viscosity, cSt**	**Dynamic viscosity, cP**
9-Jun-16	187.90	170.80	1227.96	1116.21	792.88	720.72
12-Jun-16	77.72	70.65	680.00	618.12	612.53	556.79
Density, g/ml	0.909		0.910		0.909	

4.5.4 Pressure and Flow Data - Results and Analysis for Emulsions

A description of the experimental setup is found in section 3.1.2. In the following, there is one set of data. It consisted of water-oil emulsion data before and after gas injection at different gas rates. Special attention was given to the influence of the air on pressure drop values over the tube. The flow pattern was hard to deducts without a special video recording. The densities were measured from the densitometer

and calculated from the water fraction. The densities were homogenous according to which the mixture density is a linear function of the oil or water fraction.

The experiment was performed at constant velocity, 100 cc/min. Using the empirical correlations, two flow regimes were found during the experiments: bubble flow and slug flow. At high mixture velocities (U_m> 1 m/s) the flow pattern is always slug flow. At lower velocities (U_m < 1 m/s) the flow pattern is bubble flow. The pressure drops are plotted against gas rates in **Figure 4-20**.

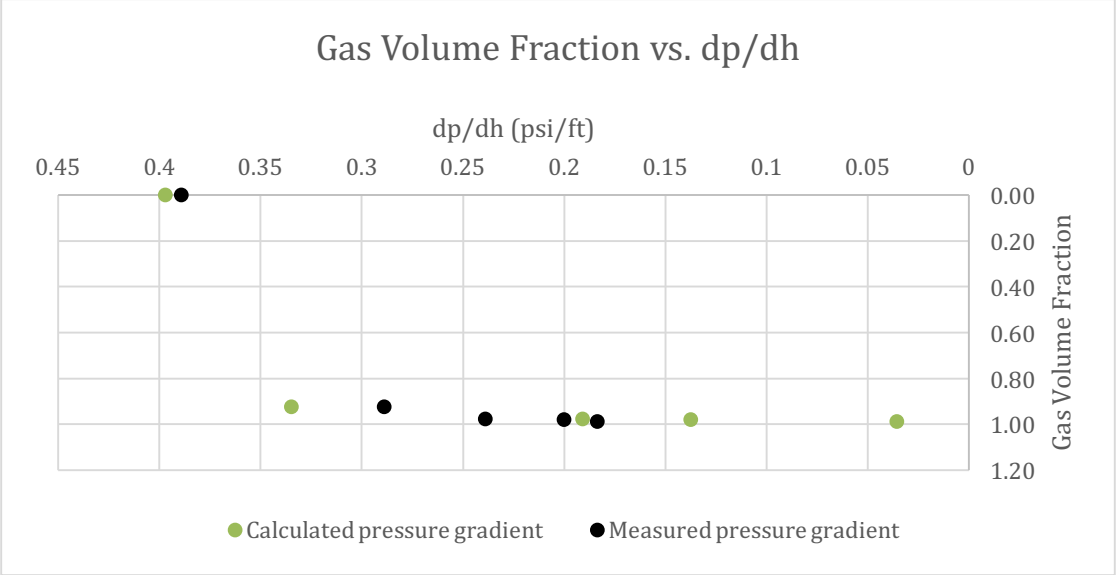

Figure 4-20 Comparison between measured and calculated pressure gradients for W/O emulsion

Chapter 5. Conclusions

The aim of this thesis was to investigate the behavior of oil water emulsion flow in a vertical tube for gas lift and ESP applications. The main focus was the effect of gas injection and centrifugal pump on emulsion stability, viscosity and pressure drops as it was a main concern in the oil field. The following are the conclusions regarding the study and suggestions for further work continuation.

5.1 Summary

The lab setup for water and oil gas lift experiments proved to work. The effect of injecting gas in a vertical pipe flow is to decrease the gravitational component of the total pressure gradient, which is the main purpose of gas lift technique. In air-water flows, the total pressure gradient is reduced since the flow is gravity dominated.

In a water-oil flow, it was proven that the injection of gas has some influence on pressure gradient. The gravitational component of the pressure gradient decreases proving the gas-lift setup is efficient.

Creating stable emulsions was achieved and water-oil emulsion was identified associated with different characteristics from water-oil emulsion. Therefore, small scale samples were created to test the stability of the emulsions. The resultant emulsion was very viscous (non-Newtonian properties were suggested). The resultant viscosity of water-oil emulsion decreased with time. The water cut used for this thesis study was 30% and 2% of mixed surfactants.

The sharp increase of the emulsion viscosity (almost tripled) was noticeable after going through the centrifugal pump and is responsible for an increase of friction

component of the pressure gradient in a vertical pipe flow. This finding confirms the effect of an ESP in boosting the formation of stable emulsion in an oil well.

The viscosity of emulsion after injecting gas had dropped significantly which is responsible for a decrease of the friction component of the pressure gradient in a vertical pipe flow. The total pressure gradient as a result was further reduced taking into consideration that the flow is gravity dominated. This is the first time such an impact is being reported.

5.2 Final Remarks and Recommendations for Work Continuation

The results displayed in this thesis give insight into the effe1`ct of the gas lift system when applied to water-oil emulsion flow as well as the influence of a centrifugal pump on water-oil emulsion properties. For this purpose, the scope of the study was limited to the available conditions at the lab.

The presence of a non-miscible fluid such as air is challenging for a comprehensive experimental investigation. The flow regime of gas in emulsion at high velocities need video imaging as well as the gas phase characteristics (local fraction, bubble size and velocity) need to be measured using an optical fibre probe or the wire-mesh technique under a careful calibration. Studying the bubble size is important because it has an effect on both the frictional and gravitational components of pressure gradient.

The up-scaling setup for real field applications depends on additional factors that were neglected in this research. For an industrial production tubing, of length higher than 1 km, the gas expansion cannot be neglected and has to be included in the pressure drop and viscosity correlations.

The thermodynamic conditions also are important parameters in real field applications. Knowing that at certain conditions of temperature and pressure can influence the solubility of natural gas in liquid phase which affect the mass and momentum balance. At large length of tube, the gas bubbles grow larger due to the gas coming out of solution and disturbing the annular or slug flow regime.

All these conditions or mechanisms can be studied in an applicable experimental facility keeping in mind the financial issues. The experimental results can be validated by creating a model for two phase flow and solving proper numerical simulations. A more complex models will involve a three phase flow models validated under similar conditions.

References

Abdel-Raouf, M. E. "Factors affecting the stability of crude oil emulsions." Crude oil emulsions–composition, stability and characterization. Croatia: Intech, Pp.183-204, 2012.

Arirachakaran, S., Oglesby, K.D., Malinowsky, M. S., Shoham, O. and Brill, J.P., "An Analysis Of Oil-Water Flow Phenomena In Horizontal Pipes ", SPE paper 1883, presented at the SPE Annual Conference and Exhibition, Oklahoma October, 1989.

Baker Hughes Oil Tools, Gas Lift catalog, available at: http://www.bakerhughesdirect.com

Bearden, J. "Electrical Submersible Pumps". Petroleum Engineering Handbook; Lake, L.W., Ed.; Society of Petroleum Engineers (SPE): Richardson, TX, Vol. 4, pp 634–720, 2006.

Becker, J.R., "Crude Oil Waxes, Emulsions, and Asphaltenes". 4th edition; Pennwell publishing company: Oklahoma, 1997.

Becher, P., "Emulsions: theory and practice," 3rd Ed.; Washington, D.C., American Chemical Society; New York: Oxford University Press, 2001.

Cairns, R.J.R., Grist, D.M., and Neustadter, E.L., "The effect of Crude oil-water interfacial properties on Water-Crude Oil Emulsion Stability," Symposium on Emulsion Technology, 1974, Academic Press inc., pp.135-151, 1996.

Clariant Oil Services, Oilfield Production Chemicals and Microbiology, 4th Edition, hts consultants, Aberdeen, 2007.

Clegg, J.D., editor. Production Operations Handbook. SPE, USA. 2007.

Clegg, J.D., Bucaram, S.M., Heln Jr., N.W., "Recommendations and Comparisons for selecting Artificial-Lift Methods", SPE 00024834, 1993.

Derjaguin, B.V. and Landau, L., "Theory of the stability of strongly charged Lyophobic sols and of the adhesion of strongly charged particles in solution of electrolytes", .Acta Physicochem. URSS, 633, 1998.

Economides, Michael J., et al. Petroleum production systems. Pearson Education, 2012.

Fleshman, R., Harryson, O.L., "Artificial Lift for High-Volume production, Oilfield Review", spring 1999.

Gary, W.S., Moshen. Z. “The practised art of Emulsion Resolution in Electrostatic Processes”, presented at Spring Meeting, Houston, 1999.

Griffin, W. C. “Classification of surface-active agents by HLB”. J Soc Cosmetic Chemists, 1, pp.311-326, 1949.

Hamaker, H.C., “The London-van der Waals attraction between spherical particles”, Physical, 1058-1072, 1997.

Heinze, L.R., Winkler, H.W., and Lea, J.F. “Decision Tree for Selection of Artificial Lift Method”, SPE 29510, 1996.

Hernandez, A. “Continuous Gas Lift Troubleshooting,” Fundamentals of Gas Lift Engineering Well Design and Troubleshooting, March 2016.

Hiemenz, P.C., “Principles of colloid and surface chemistry”, Marcel Dekker, Inc., New York, 1986

Jadid, M.B., Lyngholm, A., Opsal, M., Vasper, A., “The Pressure’s On: Innovations in Gas Lift”, Volume 18, 2006.

Johannes, K. F. “Petroleum Engineer’s Guide to Oil Field Chemicals and Fluids.” 2012.

Jones, T. J., E. L. Neustadter, and K. P. Whittingham. “Water-in-crude oil emulsion stability and emulsion destabilization by chemical demulsifiers”. Journal of Canadian Petroleum Technology 17, no. 02, 1978.

Kokal, S. “Crude Oil Emulsions: A state-of-the-art Review”, SPE paper 77497 presented at the SPE Annual Technical Conference and Exhibition, San Antonio, 29 September – 2 October, 2005.

Kokal, S.L. “Crude-Oil Emulsions”, Petroleum Engineering Handbook, SPE, Richardson, Texas, 2005.

Kokal, S., “Crude Oil Emulsions: Everything You Wanted to Know but Were Afraid to Ask”. Society of Petroleum Engineers, 2008.

Lea, J. F.;, Bearden, J. L. “ESP’s: On and Offshore Problems and Solutions”. Proceedings of the 1999 SPE Mid-Continent Operations Symposium; Oklahoma City, OK, March 28−31, 1999; SPE-52159-MS.

Lissant, K.J., “Demulsification: Industrial Application”; Surfactant science series, vol.13, Marcel Dekker: New York, 1993.

Meihack, S., “Performance of Jet Pump in the Gyda field, Internal document of

Talisman Energy Norge AS", Stavanger, 1997.

Miller, C.A., "Spontaneous emulsification produced by diffusion - a review", Colloids and Surfaces, 29 (1988) 89-102.

Miller, C.A. and Neogi, P., "Interfacial Phenomena: Equilibrium and Dynamic Effects", Marcel Dekker, Inc., New York, 1985.

Nishimi, T. and Miller, C.A., "Spontaneous emulsification produced by chemical reactions", J. Colloid Interface Sci., 237, pp. 259-266, 2001.

Opawale, A.O., "Oilfield Emulsion Control: A major issue during; A major issue during heavy crude oil production", SPE paper 128352 presented at the SPE annual conference and Exhibition, Abuja, August, 2009.

Pal, R. and Rhodes, E., "Viscosity-concentration relationships for emulsions", J. Rheol., 1021-1045, 1989.

Peña, A.A., "Dynamic aspects of emulsion stability", Ph.D thesis. Houston: Rice University, 2004.

Peña, A.A., Hirasaki, G.J. and Miller, C.A., "Solubilisation rates of oils in surfactant solutions and their relationship to mass transport in emulsions", Adv. Colloid Interface Sci., 241–257, 2006.

Richardson, J.F. and Zaki, W.N., "Sedimentation and fluidisation: Part I", Trans. Inst. Chem. Eng., 32, 1954.

Shaw, D.J., "Introduction to Colloid and Surface Chemistry", 3rd ed., Elservier Science, New York, 1992.

Schlumberger, Kikover Tools, available at: http://www.slb.com/~/media/Files/artificial_lift/product_sheets/gas-lift/kickover_tools.pdf

Schramm, L.L., "Emulsion: Fundamentals and Applications in the Petroleum Industry", Advances in Chemistry, Series-231, Washington DC, 1992

Schubert, H., and Armbroster, H., "Principles of Formation and Stability of Emulsions", International Chemical Engineering Series, No. 1, 14-28, 1992.

Singh, B.P. and Pandey, B.P, "Physical Characteristics of Natural Films formed at Crude Oil-Water interfaces", Indian Journal of Technology, Vol. 29, pp.443-447, 1991.

Stanghelle, K. U. “Evaluation of artificial lift methods on the Gyda field.” 2009.

Tadros, T.F. and Vincent, B., Emulsion stability, in “Encyclopedia of Emulsion Technology”, Marcel Dekker, Inc., New York, 1983.

Takacs, G., Gas Lift Manual, PennWell Corporation, 2005.

Taylor, G.I., “The viscosity of a fluid containing small drops of another liquid”. Prec. R. Soc. A, 41-48, 1932.

Treating oilfield Emulsions, 4th edition; Petroleum Extension service at The University of Texas at Austin: Austin, 1990.

Verwey, E.J.W. and Overbeek, J.T.G., “Theory of the Stability of Lyophobic Colloids”, Elsevier: Amsterdam, 1948.

Vrij, A. “Possible mechanism for the spontaneous rupture of thin free liquid films”, Disc. Faraday Soc., 42, pp.23-33. 1966.

Walstra, P., “Emulsion stability” Chapter 1, in Encyclopedia of Emulsion Technology’’, Becher, P., Editor. Vol.4. Marcel Dekker, Inc.: New York, 1990.

Weiss, J., Canceliere, C. and McClements D.J., “Mass Transport Phenomena in Oil-in-Water Emulsions Containing Surfactant Micelles: Ostwald Ripening”, Langmuir, Vol. 16, No. 17, 2000.

Yang, Z. L.; Sannæs, B. H.; Johnson, G. W.; Sjøvoll, M.; Schulkes, R. M. “Oil/Water Flow Experiments with Live Viscous Crude: The Influence of ESP on Flow Behavior”. Proceedings of the Offshore Technology Conference; Houston, TX, April 30−May 3, 2012; OTC- 22988-MS

Zerrouki, T., Paul, H., Monkman, J., “Expected ESP Run Life”, Internal document of Talisman Energy Norge AS, Stavanger, 2006.

Zhizhuang, J.; Bassam, Z. “ESP Operation, Optimization, and Performance Review: ConocoPhillips China Inc”. Bohai Bay Project. Proceedings of the SPE Gulf Coast Section Electric Submersible Pump Workshop; The Woodlands, TX, April 25−27, 2007; SPE-113173-MS.

Appendix A: Nomenclature

Symbols

Q	flow rate, $L^3\ T^{-1}$
TDH	total head development, L
$S.G.$	specific gravity, dimensionless
BHP	break horsepower
C	constant
WI	work interest
Q_{HC}	oil rate, $L^3\ T^{-1}$
P_{HC}	oil price
$Cost$	operational (opex) and capital (capex)
Tax	governmental taxes
NPV	net present value
P_i	injection pressure, $ML^{-1}T^{-2}$
P_d	nitrogen dome pressure, $ML^{-1}T^{-2}$
P_p	production pressure, $ML^{-1}T^{-2}$
A_d	bellows area, L^2
A_p	port area, L^2
K	ratio of dispersed phase viscosity to continuous phase
V	settling velocity, LT^{-1}
g	gravity acceleration
r	radius of the sphere, L
ΔE	change in activation energy
R	ideal gas constant
T	temperature
P_L	laplace pressure
W_e	weber number
$U(h)$	Interaction of repulsion energy
h	Height, L
V_{eff}	effective tenrminal sedimentation velocity, LT^{-1}
V_s	solids velocity, LT^{-1}
n	empirical constant
y_l	liquid holdup
V_l	liquid volume, L^3
V	pipe volume, L^3
y_g	gas holdup, void fraction
u_{sl}	liquid superficial velocity, LT^{-1}
u_{sg}	gas superficial velocity, LT^{-1}
q_l	liquid flowrate, L^3T^{-1}
q_g	gas flowrate, L^3T^{-1}
A	pipe area, L^2

u_m	mixture velocity, LT^{-1}
u_{sl}	liquid superficial velocity, LT^{-1}
$\dot{m}$	mass flowrate, L^3T^{-1}
D	pipe diameter, L
N_{vl}	liquid velocity number
N_{vg}	gas velocity number
N_D	pipe diameter number
N_L	liquid viscosity number
p	absolute pressure, $ML^{-1}T^{-2}$
p_a	atmospheric pressure, $ML^{-1}T^{-2}$
N_{Re}	reynold number
f_f	friction factor
k	length of protrusions on pipe wall, L
$\dot{m}_l$	liquid mass flowrate, L^3T^{-1}
dp	differential pressure, $ML^{-1}T^{-2}$
dz	differential height, L

Greek Symbols

η_p	Pump efficincy
μ_r	relative viscosity, $ML^{-1}T^{-1}$
μ_c	continuous phase viscosity, $ML^{-1}T^{-1}$
μ	viscosity, $ML^{-1}T^{-1}$
φ	continuous phase concentration
μ_D	dispersed phase viscosity, $ML^{-1}T^{-1}$
ρ_o	oil density, ML^{-3}
φ	dispersed phase concentration
ρ_1	density of sphere, ML^{-3}
σ	interfacial tension, MT^{-2}
ρ_2	density of medium, ML^{-3}
τ_{ext}	external stress, $ML^{-1}T^{-1}$
$\bar{\rho}$	average density, ML^{-3}
θ	angle, degrees
μ_g	gas viscosity, $ML^{-1}T^{-1}$
μ_l	liquid phase viscosity, $ML^{-1}T^{-1}$
ϵ	pipe relative roughness
ρ_l	liquid density ML^{-3}
$\gamma_{water/air}$	interfacial tension of water and air, MT^{-2}
$\gamma_{oil/air}$	interfacial tension of oil and air, MT^{-2}
$\gamma_{emulsion/air}$	interfacial tension of emulsion and air, MT^{-2}